ORIGINAL ARTICLE

Evaluation of the convection permitting regional climate model CNRM-AROME on the orographically complex island of Corsica

Virginia Edith Cortés-Hernández[1] · Cécile Caillaud[1] · Gilles Bellon[1] · Erwan Brisson[2] · Antoinette Alias[1] · Philippe Lucas-Picher[3]

Abstract

Meteorological processes over islands with complex orography could be better simulated by Convection Permitting Regional Climate Models (CP-RCMs) thanks to an improved representation of the orography, land–sea contrasts, the combination of coastal and orographic effects, and explicit deep convection. This paper evaluates the ability of the CP-RCM CNRM-AROME (2.5-km horizontal resolution) to simulate relevant meteorological characteristics of the Mediterranean island of Corsica for the 2000–2018 period. These hindcast simulations are compared to their driving Regional Climate Model (RCM) CNRM-ALADIN (12.5-km horizontal resolution and parameterised convection), weather stations for precipitation and wind and gridded precipitation datasets. The main benefits are found in the representation of (i) precipitation extremes resulting mainly from mesoscale convective systems affected by steep mountains during autumn and (ii) the formation of convection through thermally induced diurnal circulations and their interaction with the orography during summer. Simulations of hourly precipitation extremes, the diurnal cycle of precipitation, the distribution of precipitation intensities, the duration of precipitation events, and sea breezes are all improved in the 2.5-km simulations with respect to the RCM, confirming an added value. However, existing differences between model simulations and observations are difficult to explain as the main biases are related to the availability and quality of observations, particularly at high elevations. Overall, better results from the 2.5-km resolution, increase our confidence in CP-RCMs to investigate future climate projections for Corsica and islands with complex terrain.

Keywords Convection-Permitting Regional Climate Models · CNRM-AROME · CNRM-ALADIN · Hourly precipitation extremes · Sea breeze

1 Introduction

There has been an increase in weather extremes across many parts of the world over the last decades (Seneviratne et al. 2021). The Mediterranean basin, a densely urbanized region with complex and heterogeneous topography, is especially vulnerable to climate change as it warms 20% faster than the global average (Giorgi 2006). Coastal areas and islands

in this region are particularly vulnerable to severe weather (Lambert et al. 2011; Ducrocq et al. 2014), for example, to flooding and erosion due to rising sea levels, as well as an increasing frequency of intense storms caused by rising sea surface temperatures. A recent example of how climate change can intensify weather extremes (Fery and Faranda 2023; González-Alemán et al. 2023) occurred in the summer of 2022 on the island of Corsica. The western coast was hit by an unprecedented convective windstorm (i.e. Derecho) accompanied by heavy precipitation, hail and wind gusts of more than 220 km/h, causing material damage and five casualties.

To date, climate change information for vulnerability, impacts, and adaptation assessments at the regional and local scales has been provided using different methods (i.e. statistical and dynamical) to downscale Global Climate Models (GCMs), operating at resolution ~ 100 km. The

✉ Virginia Edith Cortés-Hernández
  virginia.cortes-hernandez@meteo.fr

1 CNRM, Université de Toulouse, Météo-France, CNRS, Toulouse, France

2 ClimTail, Atlantis, France

3 Département des sciences de la Terre et de l'atmosphére, Université du Québec à Montréal, Montréal, Canada

most common method is dynamical downscaling which uses a high-resolution climate model over a limited-area, often called a Regional Climate Model (RCM), to reduce the grid spacing (or increase the horizontal resolution). Until recently, due to limited computational resources, RCMs allowed for experiments at spatial resolutions ∼ 10 km (Giorgi 2019).

Compared to their driving GCMs, RCMs have a better representation of surface heterogeneities such as coastlines and topography. However, at grid spacing around 10 km, many meteorological phenomena over islands with complex topographies are not well simulated (Cronin et al. 2015; Argüeso et al. 2016; Im and Eltahir 2018). One of the reasons is that RCM spatial resolution still fails to capture the complex heterogeneity of islands (i.e. variations from coastal plains to abrupt elevations such as mountains, cliffs and valleys) and its induced atmospheric circulations, which can have a significant impact on the formation and distribution of atmospheric convection (Wu et al. 2008).

Another limitation of RCMs is the use of deep convection parameterisation schemes, which are a well-known source of model errors (Kendon et al. 2012, 2014; Fosser et al. 2015). Such errors can result in the misrepresentation of the precipitation diurnal cycle (Brockhaus et al. 2008) or in the underestimation of hourly precipitation intensities (Prein et al. 2015; Fosser et al. 2015; Ban et al. 2014). Moreover, deep convection parameterisations in RCMs are not yet able to represent precipitation extremes correctly. Indeed, many studies (Kendon et al. 2012; Prein et al. 2015; Chan et al. 2013; Ban et al. 2014; Fosser et al. 2015; Luu et al. 2022) have shown that convective parameterisations limit the representation of meteorological hazards that forms in convective environments (e.g., intense precipitation, wind gusts, hail, etc.) over mid-latitude regions. Therefore, such deficiencies in RCMs may further limit the representation of extreme events on topographically complex islands under a changing climate.

Thanks to the constant increase of computer power, some RCMs are now able to run at higher resolutions (km-scale), so-called Convection-Permitting Regional Climate Models (CP-RCMs). Mostly based on numerical weather prediction models, CP-RCMs have a spatial resolution of a few kilometres (< 4 km), in which deep convection is explicitly resolved, instead of being parameterised (Kendon et al. 2012; Prein et al. 2015). Since the early 2010, CP-RCMs have demonstrated an improved representation of complex terrains, as well as the local-scale climate processes such as extreme precipitation (Kendon et al. 2012; Ban et al. 2015; Prein et al. 2015; Kendon et al. 2017; Fumière et al. 2020; Pichelli et al. 2021; Caillaud et al. 2021; Ban et al. 2021; Luu et al. 2022; Lucas-Picher et al. 2023), and orographically induced precipitation (Adinolfi et al. 2021; Monteiro et al. 2022). These processes are particularly relevant for simulating climate conditions over islands. In fact, islands are considered ideal test beds to explore the potential of CP-RCMs due to their limited area, the presence of microclimates and the occurrence of fine-scale atmospheric processes (Lucas-Picher et al. 2021).

Climate studies using CP-RCMs over islands mainly focus on characterising rainfall. For example, the diurnal cycle of precipitation is better reproduced by CP-RCMs in terms of the phase and the amplitude (Birch et al. 2014; Argüeso et al. 2016, 2020) although with some overestimation of the intensity (Vincent and Lane 2016; Zhu et al. 2017; Wei et al. 2020; Murata et al. 2017). Other studies have shown improvements in the intensity and frequency of extreme precipitation (Kendon et al. 2012; Zhang et al. 2016; Wang et al. 2018; Dutheil et al. 2021).

The representation of topography and land–sea contrasts (i.e. coastlines, Expósito et al. 2015) is benefited by the high resolution of the CP-RCMs, and as a result, the interactions between topography and low-level winds (Morel et al. 2014; Zhang et al. 2016) are better captured. In addition, some island processes such as island rainfall enhancement (Ruppert and Chen 2020), the role of gravity waves (Ruppert and Zhang 2019; Ruppert and Chen 2020), the mechanisms driving offshore convective propagation (Barthlott et al. 2014; Coppin and Bellon 2019a, b; Hassim et al. 2016) and land–sea breeze circulations (Zhu et al. 2017; Wei et al. 2020) are also better reproduced by CP-RCMs. However, these improvements are mostly found in case studies and short simulations.

The improved representation of fine-scale atmospheric processes in CP-RCMs, mainly found for precipitation over coastal and steep regions, is expected to be beneficial for Mediterranean islands such as Corsica. To the authors' knowledge, the advantage of using CP-RCMs to simulate complex atmospheric processes that characterize Corsica island on climate scales is yet to be studied. To bridge this gap, this article will address the following scientific questions:

– Are CP-RCMs able to reproduce features of local-scale precipitation (i.e. precipitation events and extremes) over Corsica's complex orography?
– Are CP-RCMs able to represent the local-scale atmospheric circulations (i.e. sea–land breezes) in Corsica?

In order to answer these questions, this study examines different meteorological characteristics of the island of Corsica simulated by two evaluation simulations of the 2.5-km CP-RCM CNRM-AROME. These simulations are compared with their driving 12.5-km RCM CNRM-ALADIN and with different observational data sets for the 2000–2018 period.
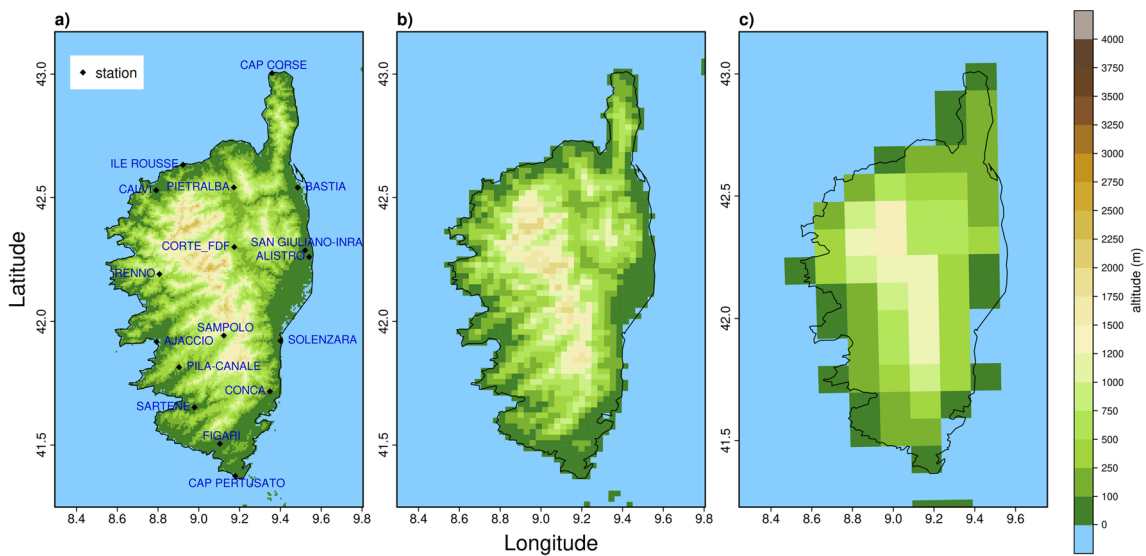
Fig. 1 **a** Location and name of the 17 weather stations (dots in black) in Corsica. Representation of the orography at different grid resolutions: **a** land elevation data from the Shuttle Radar Topography Mission (SRTM) at 90 m, **b** CP-RCM AROME at 2.5 km and **c** RCM ALADIN at 12.5 km
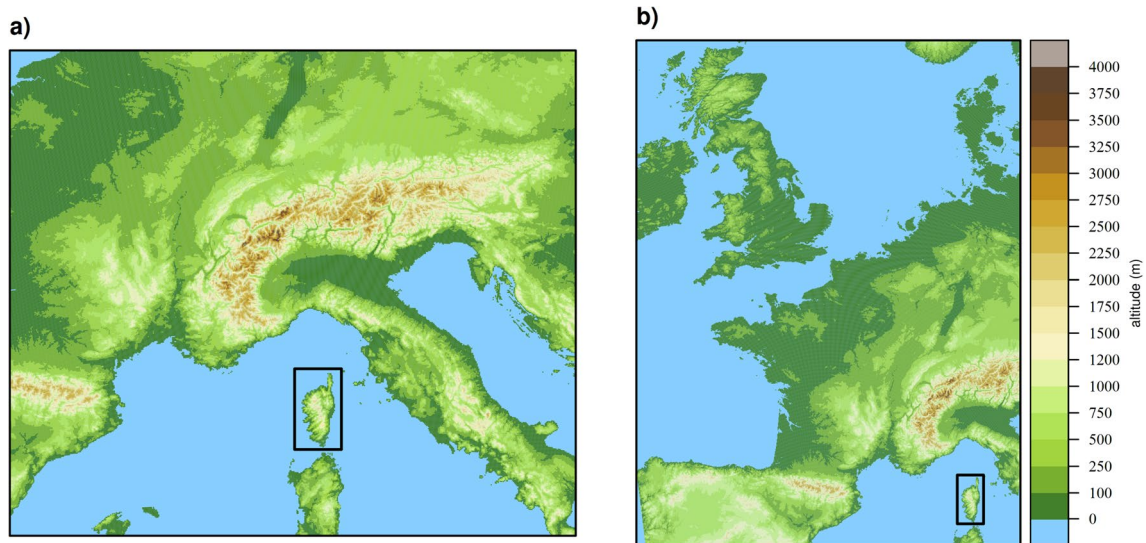
Fig. 2 Domains of the CP-RCM AROME simulations including Corsica (black rectangle): **a** AROME ALP and **b** AROME NWE

Section 2 describes the study region and its associated meteorological phenomena, the observational data sets, and the model simulations. Section 3 presents the methods. Section 4 shows the results of the model evaluation in reproducing different features of precipitation and local circulations (e.g. hourly precipitation extremes, precipitation events, and sea breezes). General discussion and conclusions are given in Sect. 5.

2 Study region, data and simulation set-up

2.1 The island of Corsica

Figures 1 and 2 show the study region. Located in the north-western Mediterranean Sea, north of the Sardinia island and south-east of continental France, Corsica is the 4th largest Mediterranean island (area of 8 722 km) with an extension from north to south of about 180 km and from

west to east of about 80 km and with about 1000 km of coastline. It is part of Metropolitan France with a population of 351 300 inhabitants (INSEE 2023[1]). This island has a complex orography with steep slopes and deep valleys (Fig. 1a). More than 60% of its surface is covered by mountain ranges (mainly located on the northwestern side) with some of them higher than 2000 m and the highest summit of 2706 m (Monte Cinto). Such topographic variations generate differences in Corsica's climate and vegetation (Rome and Giorgetti 2007).

According to the Köppen climate classification, Corsica has a predominantly Mediterranean climate, as it is surrounded by a relatively warm sea and with some subtropical climate characteristics, for example, hot summers and mild winters. However, at high elevations (> 800 m), Corsica presents Alpine climate characteristics with lower temperature, significant diurnal and annual thermal variability, an increase in precipitation with rainy and snowy precipitation, and winds strongly conditioned by the local relief (Rome and Giorgetti 2006). Corsica's climate is also affected by prevailing Mediterranean regional winds coming from the southwest (Libeccio), west-northwest (Mistral), east (Levante), northeast (Grecale) and north (Tramonte). This island has a sufficient landmass size (i.e. able to cause a significant land–sea contrast) and steep mountain ridges that favour the formation of precipitation (Barthlott and Kirshbaum 2013; Knerr et al. 2020). Annual precipitation regimes vary from coastal regions (i.e. 500 mm/year) to mountain altitudes (> 1500 mm/year).

Moreover, Corsica is often affected by severe weather, e.g. heavy precipitation, floods, windstorms, Saharan dust events, waves and coastal erosion, droughts, forest fires and lightning (Lambert et al. 2011; Scheffknecht et al. 2016). Due to its geographical position, this region is considered ideal for the study of intense precipitation in the Mediterranean and was part of the research program MISTRALS (Mediterranean Integrated STudies at Regional And Local Scales[2]), which was dedicated to improving the understanding of the Mediterranean Basin environmental process and its evolution under global climate change. This included the HyMeX (Hydrological cycle in Mediterranean Experiment[3]) research programme, which focuses on high-impact weather events and their predictability, and the ChArMEx (The Chemistry-Aerosol Mediterranean Experiment[4]) research project which investigates Mediterranean regional chemistry-climate interactions. More specifically for Corsica, the CORSica (Corsican Observatory for Research and Studies

on Climate and Atmosphere-ocean environment) project setup a multiparametric observation platform (Lambert et al. 2011), which facilitated exchanges between HyMeX and ChArMEx. More recently, the EXAEDRE (EXploiting new Atmospheric Electricity Data for Research and the Environment) project launched a dedicated field campaign over Corsica to measure the electrical activity in thunderstorms (Erdmann et al. 2020). All the above initiatives aimed at providing valuable weather and climate information on a region that has not been exhaustively documented.

2.2 Mediterranean heavy precipitation events

During late summer and autumn, devastating heavy precipitation events (HPEs) take place in the western Mediterranean region, in particular in southeastern France and Corsica producing precipitation amounts that can exceed 200 mm in a few hours (Ducrocq et al. 2008; Nuissier et al. 2008, 2011; Caillaud et al. 2021). Then from November to February, the Gulf of Genoa (just north of Corsica) becomes an active cyclogenesis region and the nearby Corsica region registers a high cyclone track density (Flaounas et al. 2023; Trigo et al. 2002). HPEs have been studied in the framework of the HyMeX (Drobinski et al. 2014; Ducrocq et al. 2014) and the main results have helped to identify several factors responsible for their occurrence (Khodayar et al. 2021): (i) instability and moisture supply from the evaporation coming from the Mediterranean Sea after the warm season, (ii) slow-evolving synoptic-scale conditions and (iii) deep convection triggered by orographic lifting, cold-pool or mesoscale low-level convergence.

Long-duration HPEs affecting Corsica are mainly associated with quasi-stationary convective systems, high CAPE values and a moist troposphere coming from the south of Corsica with a predominant southerly flow in the boundary layer (Ricard et al. 2012). A 31-year (1985–2015) climatology of HPEs (precipitation > 100 mm/day) by Scheffknecht et al. (2017) found a total of 173 events (i.e. about 6 HPEs per year), with more than half of HPEs occurrence observed from September to December (with October being the most active month), and a few during summer (i.e. 10 events).

In the last decade, CP-RCMs have provided insight into precipitation extremes, especially on the location and structure of Mediterranean HPEs, for example, in the eastern Mediterranean coast and the Island of Cyprus (Armon et al. 2020), Southeastern France (Fumière et al. 2020; Luu et al. 2022), the Catalonia coast (Meredith et al. 2020), the pan-Europe region (Berthou et al. 2020), the pan-Alpine region (Caillaud et al. 2021; Ban et al. 2021; Pichelli et al. 2021) and the Northwestern Europe region (Lucas-Picher et al. 2023); all these have demonstrated an added value of CP-RCMs in comparison to RCMs. Such benefits are partly associated with the increased grid resolution, which allows a

---

more realistic representation of surface heterogeneities such as land–sea contrasts and topography but more importantly because deep convection is explicitly resolved by CP-RCMs.

2.3 Local winds: sea–land and valley–mountain breezes

During summer, sea breezes are mainly predominant on the eastern and western Corsica coastlines. They developed during the daytime, under relatively clear skies and under a weak synoptic forcing, and are generally stronger than the nighttime land breezes. Also, sea breeze wind speed seems to be stronger on the west coast compared to the east coast, probably associated with the shape of the bays (Knerr et al. 2020). Together with the local evaporation, moisture supply over islands is controlled by sea breezes which constitute the main low-level mesoscale circulation during summer for the western Mediterranean coast (Azorin-Molina et al. 2011).

On mountain islands like Corsica and Sardinia, sea breezes and valley winds can combine to form an extended sea breeze, which can favour the initiation of atmospheric convection (Kottmeier et al. 2000; Barthlott et al. 2014; Leps 2016; Furberg et al. 2002). Extended sea breezes occur when sea breezes and valley winds blow in the same direction inducing stronger wind speeds, increasing the probability of developing deep convection over elevated areas (Kondo 1990). Furthermore, sea breezes can interact with regional winds. For example, the Mistral (strong northerly wind) can inhibit the inland sea-breeze penetration in southern France. In addition, the steep topography of vicinity islands such as Sardinia can also block the arrival of maritime air (Barthlott and Kirshbaum 2013).

The accurate representation of local circulations over complex regions is still a challenge in climate modelling. Few studies using CP-RCMs consider shorter simulation periods. For example, in a study by Langhans et al. (2013), the diurnal evolution of the thermally driven flows (particularly valley winds), cumulus formation, and surface precipitation were well-captured by two CP-RCMs at 1 and 2-km horizontal resolution over the European Alps during an 18-day summer period. A sensitivity case study by Barthlott and Kirshbaum (2013) using a 2.8-km horizontal resolution CP-RCM, found an enhancement of convective precipitation influenced by terrain height in Corsica and Sardinia islands. Moreover, CP-RCM simulations of two cases with nocturnal offshore convection in Corsica emphasise that convective initiation is very sensitive to model initialisation time and the representation of terrain elevation (Barthlott et al. 2014). A more recent study by Zhu et al. (2021) over a tropical island in South China, demonstrates an adequate agreement between a

3-km CP-RCM and radar observation for a 3-year period in reproducing spatial characteristics of convection initiation linked to local circulations and low-level large scale flows.

2.4 Description of the observational datasets

Two types of observational datasets are considered in this study:

– Weather station data is available through the BDClim (Base de Données CLIMatologiques) database of Météo-France. For precipitation, a total of 17 weather stations in Corsica were selected considering hourly data frequency and high-quality and near-continuous data for the 2000–2018 period (Fig. 1a). However, most of the stations are spread and located on the coast, and only three stations are at altitudes above 500 ms. The station with the highest elevation at 837 m is located at Sampolo. Although there are a few stations found at higher elevations, they have discontinuous and low-quality data and are therefore not suitable for the purpose of this study. For wind, 16 weather stations with hourly observations were used.
– Gridded precipitation datasets: COMEPHORE and PRESCILIA

COMEPHORE (COmbinaison en vue de la Meilleure Estimation de la Précipitation HOraiRE) is a 1-km gridded dataset of hourly precipitation for the Metropolitan France region developed by Météo-France (Tabary et al. 2011; Fumière et al. 2020). This database is based on the combination of available radar and rain gauge observations. However, in addition to the low density of stations at high elevations over Corsica, the radar coverage is rather poor. Until recently, there was only one precipitation radar in Corsica, on its eastern coast. With the masking effect from mountains, the quality of the radar coverage on the west coast was considered low. However, since 2018, a radar installed in Ajaccio has improved the radar coverage on the west coast. Unfortunately, this duration is therefore no longer enough to be considered in this study. Such limitations are likely to affect the comparison of model simulations and observations, particularly for precipitation over mountainous areas (> 1500 m), which tends to be underestimated (Caillaud et al. 2021).

PRESCILIA (PREcipitations Spatialisées Contraintes par une InitiaLIsation Aurelhy) is a 1-km daily gridded precipitation dataset developed at Meteo-France based on a geostatistical method that considers rain gauges data and the Aurelhy climatology by weather type (Soubeyroux

et al. 2019). Aurelhy is based on a method of co-kriging station data with regression of elevation parameters. Therefore, PRESCILIA includes an altitude correction on precipitation data, which is not present in the COME-PHORE dataset. However, PRESCILIA is only available at daily time-step.

In addition, land elevation data from the Shuttle Radar Topography Mission (SRTM)[5] was used to create a land–sea mask which facilitates the evaluation of land-only model simulation results.

2.5 Description of climate models

In this study, climate simulations over Corsica are performed by:

– The CP-RCM CNRM-AROME (from now on CP-RCM AROME) cycle 41t1 is a bi-spectral non-hydrostatic lim-ited-area climate model with a semi-lagrangian advec-tion scheme and a semi-implicit time discretisation. Due to its high horizontal resolution (2.5 km), AROME is able to explicitly resolve deep convection, thus deep convection parameterisations are turned off. It is based on the numerical weather prediction (NWP) model of Météo-France AROME (Applications de la Recherche á l'Opérationnel á Méso-Echelle) (Seity et al. 2011) and has been used for almost a decade at the CNRM (Centre National de Recherches Météorologiques) for climate purposes (Fumière et al. 2020; Caillaud et al. 2021; Lucas-Picher et al. 2023).
– The RCM CNRM-ALADIN (from now on RCM ALA-DIN) version 6 is a bi-spectral, hydrostatic limited-area climate model with a semi-lagrangian advection scheme and a semi-implicit time discretisation with parameter-ised deep convection (Nabat et al. 2020; Piriou et al. 2007; Guérémy 2011). It is also based on the NWP model ALADIN (Aire Limitée Adaptation dynamique Développement Inter-National).

2.6 Description of the simulations set-up

Two hindcast simulations, i.e. evaluation simulations at a 2.5-km grid resolution driven by a reanalysis, of the CP-RCM AROME were performed over two domains (Fig. 2) that cover the region of study. To avoid a large resolution jump, an intermediate RCM at 12.5-km grid resolution is used to drive the CP-RCM AROME. Therefore, the RCM CNRM-ALADIN is driven every 6 h by the ERA-Interim reanalysis. In turn, CNRM-ALADIN forces the CP-RCM AROME every hour. After removing a 2-year spin-up,

these simulations comprise a common 19-year (2000–2018) period. The two AROME simulations were carried out with the same version of the model, but performed on two dif-ferent domains:

(a) ALP-3 is the common pan-Alpine domain (from now on AROME ALP) defined for the CORDEX (Coordinated Regional Climate Downscaling Experiment) FPS-Convec-tion (Flag Pilot Study on Convection) project (Coppola et al. 2020). AROME ALP simulation (Fig. 2a) is driven by the RCM ALADIN on the MED-CORDEX domain (not shown) (from now on ALADIN MED (Ruti et al. 2016)). The ALADIN MED simulation uses spectral nudging (Radu et al. 2008) to guide further large-scale conditions.

(b) NWE-3 is the Northwestern European domain (from now on AROME NWE) established for the EUCP (European Climate Prediction) project H-2020 (Horizon 2020, http://www.eucp-project.eu). AROME NWE simulation (Fig. 2b) is driven by the RCM ALADIN on the EURO-CORDEX domain (not shown). For AROME NWE, Corsica is located rather close to the bottom right corner of the domain, poten-tially impacting the climate simulations. However, initial validation indicates that this impact is low (Lucas-Picher et al. 2023).

For the surface boundary conditions, the Sea Surface Temperatures (SSTs) come from interpolated monthly ERA-Interim SSTs (around 80 km) as recommended in the CORDEX-FPS on Convection simulation protocol. Since the Mediterranean Sea plays an important role in the climate of Corsica, supplying moisture and convective instability dur-ing HPEs and in fine-scale interactions occurring between the low-level atmosphere and the ocean mixed layer (Leb-eaupin Brossier et al. 2008; Rainaud et al. 2017; Bouin and Lebeaupin Brossier 2020); the lack of sub-monthly varia-tions and the coarse spatial resolution SSTs are likely to influence the representation of rainfall characteristics in climate model simulations.

For the radiative forcing, the Nabat et al. (2013) aerosols dataset provides monthly evolutionary two-dimension maps for dust, sea salt, organic carbon and black carbon and yearly and monthly evolutionary two-dimension maps for sulfates. However, the sulfate forcing is not present in the AROME ALP simulation due to an error in the preparation of the simulation. More details concerning the configuration of the models can be found in Table 1.

3 Methods

3.1 Selection of grid cells in models simulations

For a local evaluation, observations of the 17 weather sta-tions in Corsica were compared to the selected neighbour grid cell in COMEPHORE, AROME and ALADIN. Thus,

---

[5] http://srtm.csi.cgiar.org.

Table 1 Configuration of the climate simulations

Model	CP-RCM		RCM	
	CNRM-AROME	CNRM-AROME	CNRM-ALADIN	CNRM-ALADIN
Simulation	AROME ALP	AROME NWE	ALADIN MED	ALADIN EUR
Domain	ALP-3	NWE-3	MEDCORDEX	EUROCORDEX
Version	41t1	41t1	6	6
Horizontal resolution	2.5 km	2.5 km	12.5 km	12.5 km
Vertical levels	60	60	91	91
Initial and lateral boundary conditions	CNRM-ALADIN 6	CNRM-ALADIN 6	ERA-Interim 80 km	ERA-Interim 80 km
Coupling frequency	1 h	1 h	6 h	6 h
SST coupling	ERA-Interim monthly	ERA-Interim monthly	ERA-Interim monthly	ERA-Interim monthly
Aerosols	Nabat et al. (2013)	Nabat et al. (2013)	Nabat et al. (2013)	TACTIC V2 (Michou et al. 2020)
Spectral nudging	No	No	Yes	No

Table 2 Location of the 17 stations in Corsica and their corresponding altitude and land surface fraction, which are obtained from the selected grid cell in AROME ALP, AROME NWE, ALADIN MED and ALADIN EUR simulations

Location	Altitude (m)					Land surface fraction (%)			
	Weather station	AROME ALP	AROME NWE	ALADIN MED	ALADIN EUR	AROME ALP	AROME NWE	ALADIN MED	ALADIN EUR
AJACCIO	5	16.2	25.8	190.3	248.4	97	97	100	100
BASTIA	10	5.3	8.4	60	228.5	97	94	57.6	100
SOLENZARA	12	39.7	28.8	82.3	579	92	87	57	100
FIGARI	20	26.6	17.8	164	249	96.3	91.4	100	100
SAN GIULIANO	47	67.8	31	195.3	170	100	100	57.4	100
CALVI	57	74.5	77.4	262.7	344	95	91.8	100	100
SARTENE	62	145.7	153.3	356.7	372	100	100	100	100
ALISTRO	65	21.4	40.8	195.3	170	100	100	57.4	100
CAP CORSE	72	206	196	183	299	100	92	48	75
CAP PERTU-SATO	107	61	65.2	7.8	46	100	91.7	100	74.5
ILE ROUSSE	142	204.6	227	101.9	344	100	95	60.6	100
CONCA	253	104	211	596	530	100	100	100	100
CORTE	362	394.8	410.7	670.4	860	100	91.4	100	100
PILA-CAN-ALE	407	367.8	296	524.4	248.3	100	100	100	100
PIETRALBA	510	502.8	490	557	608.6	100	100	100	100
RENNO	755	543.5	706.7	476.7	886.5	100	100	100	100
SAMPOLO	837	724	890.8	1115.7	1315.9	100	100	100	100

the surface level parameters in AROME and ALADIN, orography and land–sea mask, are used to identify the adequate grid cell.

The most representative grid cells were selected following three criteria: (1) the closest grid cell using the minimum spatial distance between the gridded data set and the weather station location, (2) the land surface fraction value higher than 50%, and (3) the altitude value closest to the weather station.

Corresponding altitude and land surface cover values of the chosen grid cells are displayed in Table 2. Given the complex topography of Corsica, the choice of the appropriate grid cells of 12.5-km ALADIN was sometimes difficult. For example, Cap Corse is a rocky barrier 37 km long and between 10 and 14 km wide. Therefore, the choice of the grid cell for the Cap Corse station for ALADIN was complicated and required an exception to the selection rules: for this station, the corresponding land surface fraction value for ALADIN MED

selected grid cell is only 48% as the neighbouring grid cells have smaller values.

3.2 Interpolation

For the spatial analysis of precipitation, gridded datasets at different resolutions including COMEPHORE (1 km), PRESCILIA (1 km), AROME (2.5 km) and ALADIN (12.5 km) are interpolated to a common 3-km grid resolution using the cdo first order conservative remapping (Ban et al. 2021; Pichelli et al. 2021; Caillaud et al. 2021).

3.3 Probability density function of hourly precipitation

The Probability Density Function (PDF) is used to investigate the whole distribution of hourly precipitation in autumn, i.e. the wettest season in Corsica.

The frequency of hourly precipitation is split into multiple irregular bins, which are calculated using the following expression:

$$bins = \left\{ \left(\frac{i}{5} \right)_{i=1,...,5}, 2^{\left(\frac{j}{3} \right)_{j=1,...,20}} \right\}. \tag{1}$$

In this study, a total of 25 bins ensure that the largest precipitation values are represented. Then, the mean precipitation for each bin was computed. Results are presented in Sect. 4.5.

3.4 Root mean square error

The root mean square error (RMSE) is commonly used to measure the difference between predicted (i.e. each model simulation) values and observed ones. RMSE is always positive, values closer to zero indicate a good match and higher values indicate higher differences. However, RMSE is scale-dependent and sensitive to outliers.

$$RMSE = \sqrt{\sum_{i=1}^{n} \frac{(s_i - o_i)^2}{n}} \tag{2}$$

where s is the model simulation, o is the observational data set and n is the sample size. Results are shown in Sects. 4.2, 4.3 and 4.4.

3.5 Skill score

The mean square skill score (MSSS), adapted from Murphy (1988), is implemented to evaluate and compare the performance of the CP-RCMs simulation to their parent simulations. The MSSS is defined as follows:

$$MSSS = 1 - \frac{\sum_{i=1}^{n}(s_i - o_i)^2}{\sum_{i=1}^{n}(r_i - o_i)^2} \tag{3}$$

where s is the model simulation AROME, o is the observational dataset (COMEPHORE), r is the reference dataset ALADIN (parent nest of AROME), i is a specific grid point, and n is the total number of grid points. A weighting function (w) can be included, but for this study, it is set to 1. The implementation of the MSSS facilitates a direct comparison of the datasets' performances. The MSSS is 1 when AROME perfectly aligns with the observations, between 0 and 1 when AROME surpasses ALADIN, and below 0 when ALADIN outperforms AROME. Thus MSSS enables the quantification of the added value of AROME compared with ALADIN. Results can be found in Sects. 4.2, 4.3 and 4.4.

4 Results: added value of the CP-RCM AROME over Corsica

4.1 Annual cycle of precipitation

Figure 3 shows the mean annual cycle of daily precipitation for eight selected locations in Corsica: Calvi, Ajaccio, Pila-Canale and Figari (western Corsica), Cap Corse, Bastia and Solenzara (eastern Corsica) and Sampolo (central and mountainous Corsica). The annual cycle of precipitation presents a predominant Mediterranean regime characterised by a dry summer and a wet season with two main peaks, one at the end of autumn and the other at the end of winter. However, mountainous regions in Corsica (e.g. Sampolo) have a predominant Alpine regime with a wetter summer and a wetter winter season with higher precipitation intensities, which are almost double compared to coastal areas.

The comparison of the annual cycle of precipitation between the observational data COMEPHORE and the weather stations shows a general agreement, but some differences were also identified. For example, COMEPHORE overestimates daily mean precipitation in Cap Corse during the autumn months. The annual cycle of precipitation is also captured by simulations from AROME and ALADIN. Results from AROME show an overall better representation in comparison to ALADIN, which tends to overestimate the wettest months. Few differences were found between AROME ALP and NWE: for example, the annual cycle is better captured in AROME ALP for Calvi, Ajaccio and Solenzara and in AROME NWE for Figari and Pila-Canale. However, significant differences can be seen in ALADIN MED and ALADIN EUR with respect to the observations and this is probably due to the spectral nudging in ALADIN MED. Moreover, daily precipitation is overestimated by ALADIN and AROME
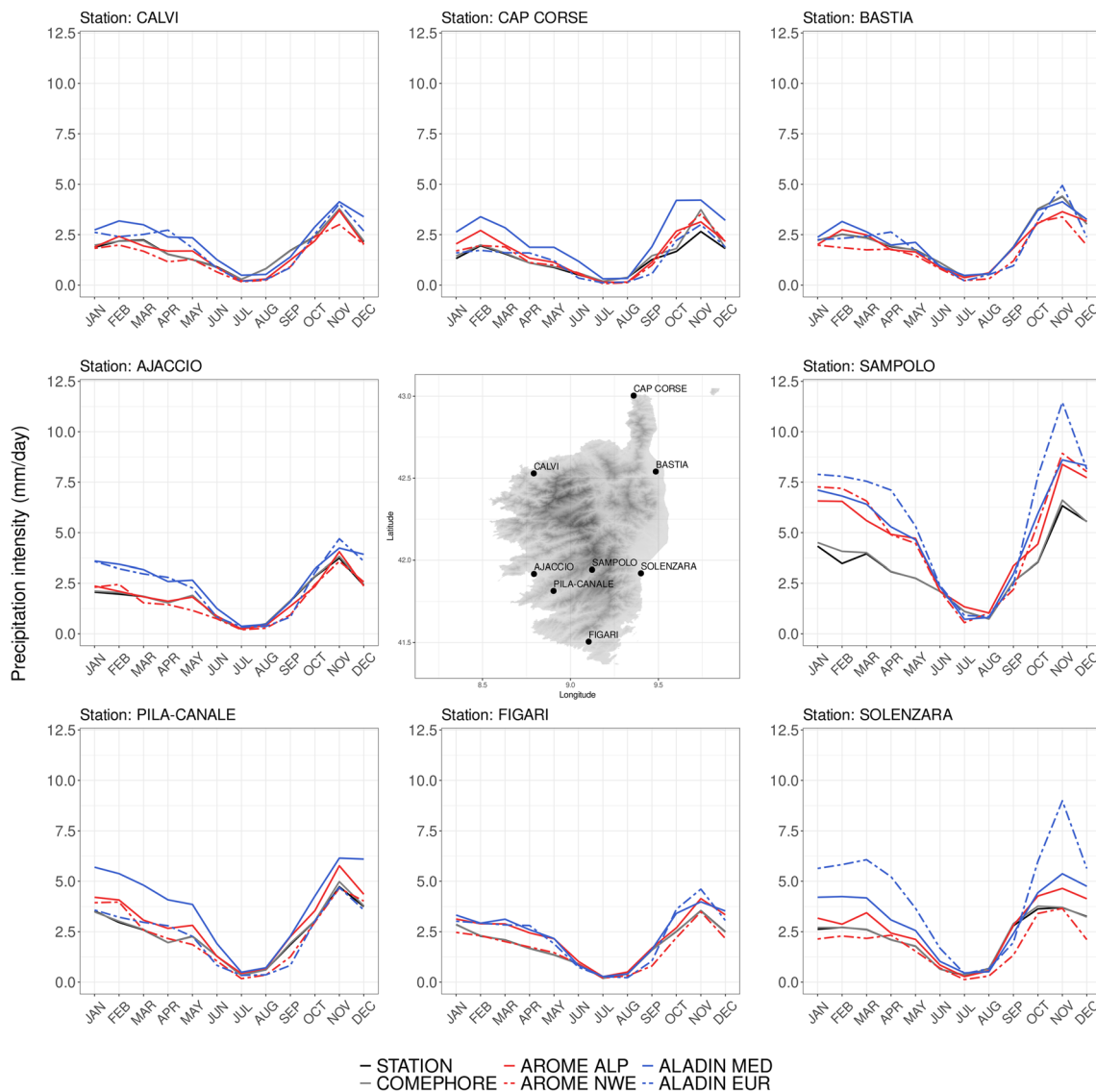
Fig. 3 Mean annual cycle of precipitation (mm/day) during the 2000–2018 period for COMEPHORE (grey), AROME ALP (red), AROME NWE (dashed red), ALADIN MED (blue), ALADIN EUR (dashed blue) and STATION (black) for eight locations in Corsica: Calvi, Ajaccio, Pila-Canale, Cap Corse, Figari, Bastia, Sampolo and Solenzara

for Cap Corse and the highest elevation station Sampolo. This overestimation is particularly found in ALADIN EUR and could be influenced by the selection of the grid point in the model.

4.2 Seasonal mean of daily precipitation

The seasonal mean of daily precipitation is analysed for the region of study (Fig. 4). For this, two observational gridded data sets (COMEPHORE and PRESCILIA) are compared with the climate simulations (AROME ALP, AROME NWE, ALADIN MED and ALADIN EUR). The climate characteristics of Corsica are identified in the observations. The underestimation of COMEPHORE at high altitudes seems

at least partly improved by the altitude correction included in the PRESCILIA dataset, which can be considered more reliable. The main precipitation features in the observation datasets are realistically represented by all model simulations. This skill is largely due to the boundary conditions imposed by the large-scale atmospheric circulation that leads to realistic seasonal regimes. However, at high elevations (> 800 m) and especially during wet months (e.g. DJF and SON), AROME simulations show localised higher precipitation intensities (in reddish) that are almost double those of the observations. Simulations of ALADIN also show higher precipitation (in yellow and orange) over more extended areas which is probably due to the shape of the ranges (slopes and heights) being underrepresented by their
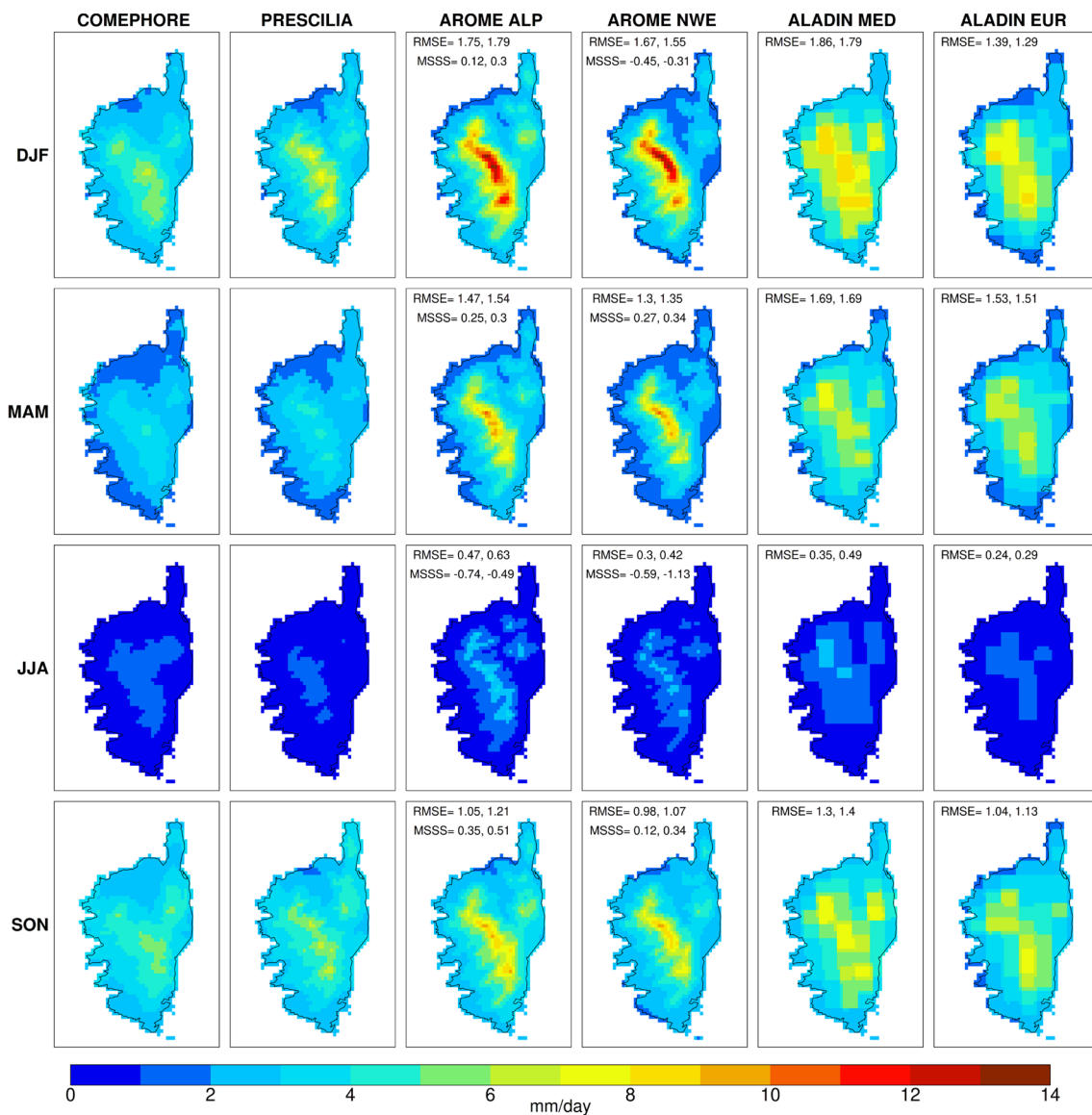
Fig. 4 Spatial distribution of the seasonal mean of daily precipitation (mm/day) for COMEPHORE, PRESCILIA, AROME ALP, AROME NWE, ALADIN MED and ALADIN EUR for the 2000–2018 period. The RMSE and the MSSS indicate the performance of model simulations, where left interval values correspond to the comparison with COMEPHORE and right interval values for PRESCILIA

coarse resolution. The highest RMSE magnitudes are found for ALADIN MED while the lowest for both AROME NWE (MAM and SON season) and ALADIN EUR (DJF and JJA, the wettest and driest season, respectively). When comparing AROME to ALADIN using the MSSS, there is indeed an improved representation by AROME particularly for wet months (positive MSSS values, except for AROME NWE in winter). However, for the driest summer season, there is an overestimation by AROME (negative MSSS values) that can not be properly quantified due to limitations in the observations.

To better understand such differences, daily mean precipitation was associated with the elevation in Corsica, as shown in Fig. 5. This plot shows the seasonal daily precipitation (mm/day) related to 150-m elevation intervals (from 0 to 2400 m) obtained for COMEPHORE, PRESCILIA, AROME ALP, AROME NWE, ALADIN MED and ALADIN EUR. Results show an overall gradual increase in daily precipitation with height. When compared, COMEPHORE shows a lesser gradual increase while all simulations indicate a steep increase (especially for ALADIN MED). The coarse resolution of ALADIN limits this comparison up to 1350 m. Although the increase in precipitation with height is higher in PRESCILIA (using a correction with the elevation) than in COMEPHORE, this is still lower than the one simulated. It is difficult to determine whether the magnitude
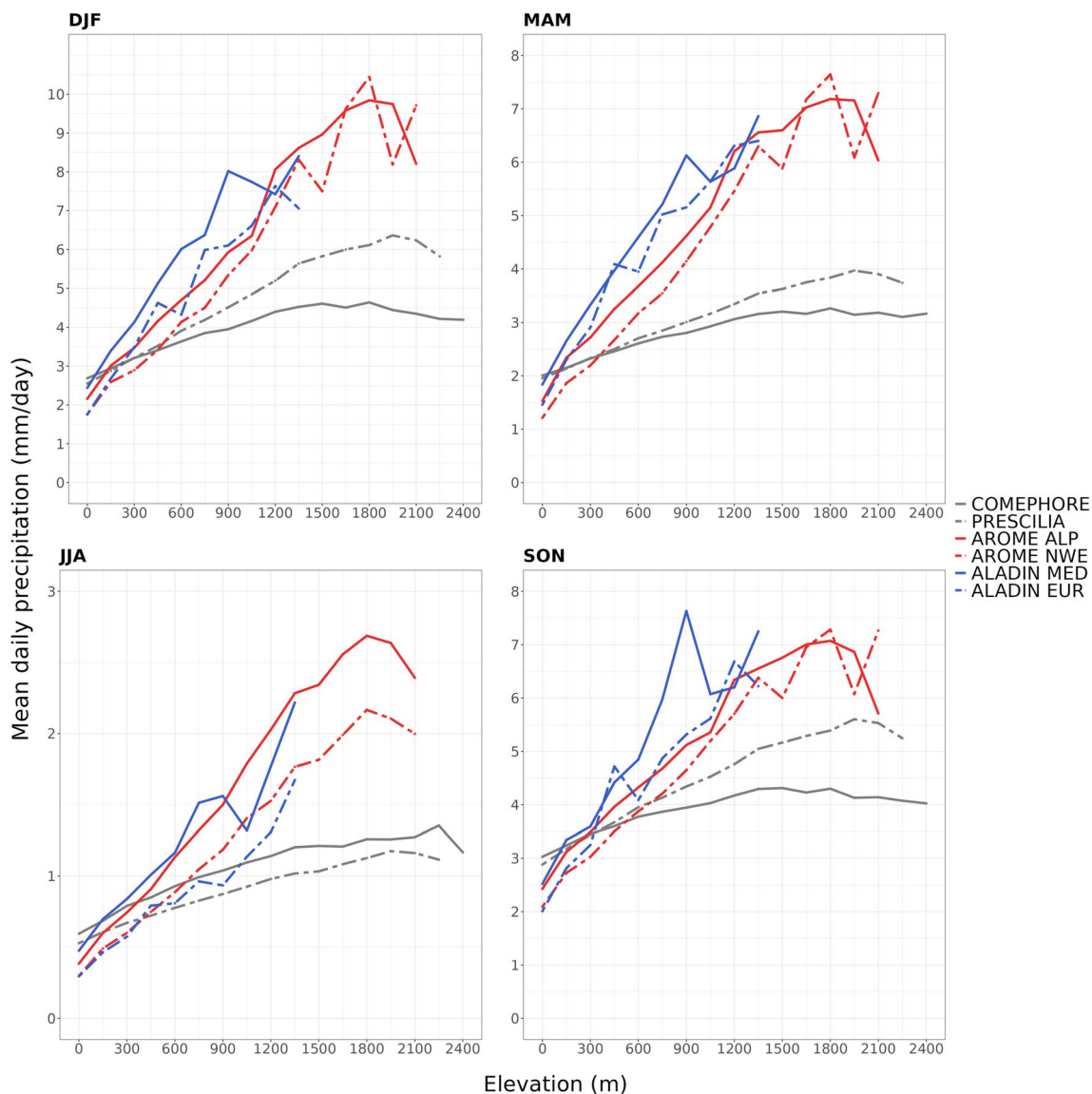
Fig. 5 Seasonal daily precipitation (mm/day) associated with mean elevation intervals for COMEPHORE (grey line), PRESCILIA (grey dashed line), AROME ALP (red line), AROME NWE (red dashed line), ALADIN MED (blue line) and ALADIN EUR (blue dashed line). Mean elevation consists of 150-m continuous intervals

of precipitation over mountain ranges is overestimated by the model simulations or the observational datasets underestimate precipitation due to deficiencies in the observations related to precipitation under-catch, especially during the snowy and windy winter season, a partial radar coverage, and the low density of weather stations (Lundquist et al. 2019). It seems fair to say that the observations have limitations and probably underestimate precipitation. Moreover, the effect of orographic precipitation which is sometimes overestimated by RCMs, seems generally overestimated by CP-RCMs.

4.3 Summer diurnal cycle of precipitation

During summer, strong land–sea contrasts between the landmass of Corsica and the surrounding waters lead to significant sea breezes, especially on the west and east coasts. Local topography has an important regulating effect on the sea-breeze: influencing the inland penetration, affecting convergence/divergence, controlling the number of sea-breezes and their onset time (Abbs and Physick 1992). A study by Mahrer and Pielke (1977) found that the sea breeze combined with mountain circulations produced a more intense circulation (than if acting separately) able to reach the lee side of the mountains in the early afternoon. This interaction
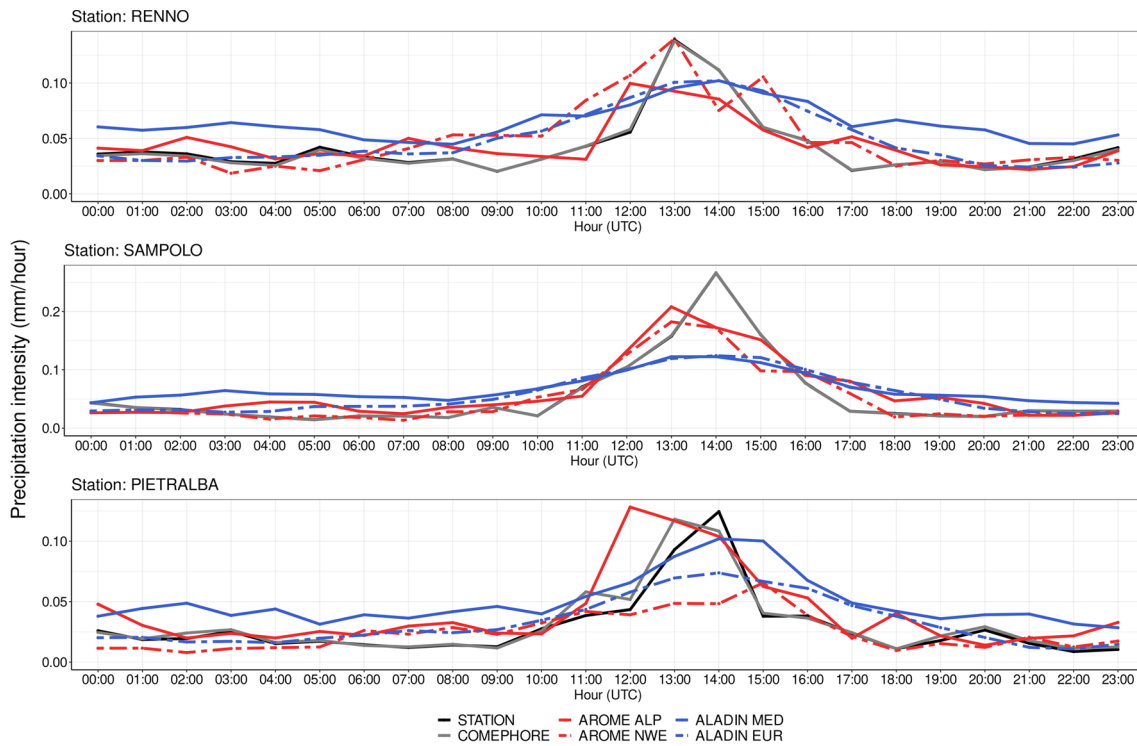
Fig. 6 Summer diurnal cycle of precipitation for COMEPHORE (grey), AROME ALP (red), AROME NWE (dashed red), ALADIN MED (blue), ALADIN EUR (dashed blue) and STATION (black) at three locations: Renno (top), Sampolo (middle) and Pietralba (bottom)
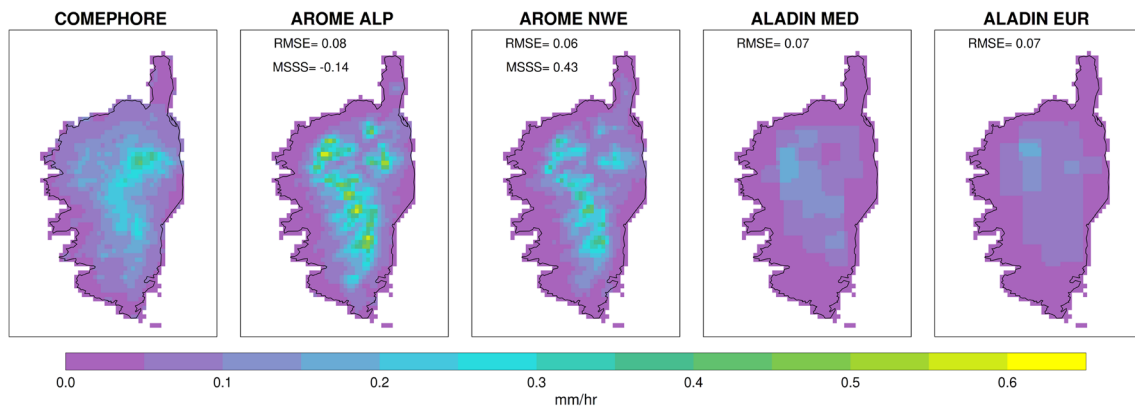
Fig. 7 Amplitude of the summer diurnal cycle of precipitation over Corsica for COMEPHORE, AROME ALP, AROME NWE, ALADIN MED and ALADIN EUR. The corresponding RMSE and the MSSS values are included

can also influence the diurnal cycle of precipitation. Figure 6 shows the summer diurnal cycle of precipitation at three locations close to the centre of the island: Renno (775 m), Sampolo (837 m) and Pietralba (510 m). The observed diurnal cycle of precipitation for COMEPHORE and the weather stations are in good agreement for the three locations. It reaches an early afternoon peak (at 1300 or 1400 UTC). This feature is better captured by the AROME simulations compared to ALADIN. However, AROME shows sometimes

a peak that is 1–2 h earlier compared to that of the observations. Despite this, the AROME simulations demonstrate a better representation of the amplitude of the diurnal cycle whereas ALADIN simulations depict a peak with a lower amplitude. AROME ALP also shows a better representation of the amplitude (e.g. Sampolo) than AROME NWE. For the other stations, mostly located on the coast, mean hourly precipitation values are much lower, and therefore no clear diurnal cycle of precipitation was identified (not shown).
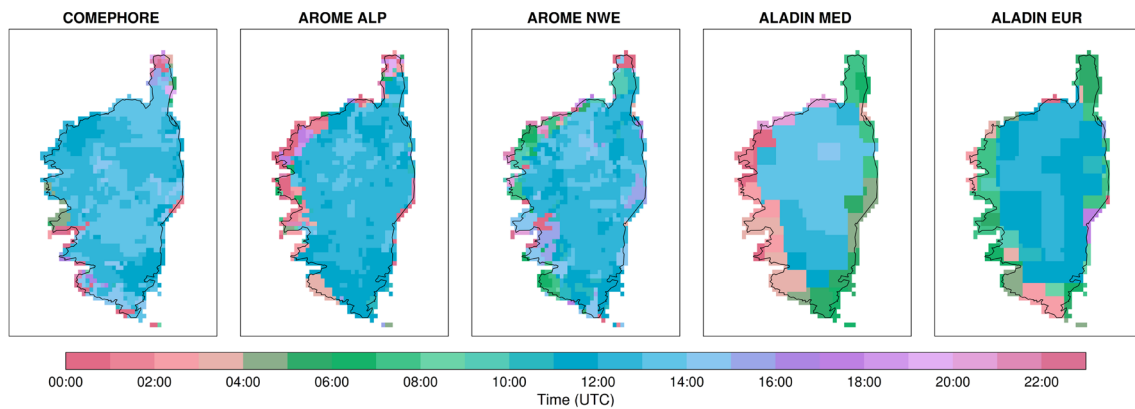
Fig. 8 Time (in UTC) of the maximum of the diurnal cycle of precipitation in summer for COMEPHORE, AROME ALP, AROME NWE, ALADIN MED and ALADIN EUR

The summer diurnal cycle of precipitation is further investigated over the entire Corsica in each grid point and in terms of the amplitude (difference between the maximum and minimum precipitation intensity) and time of hourly maxima. Figure 7 shows the amplitude of the summer diurnal cycle for COMEPHORE, AROME ALP, AROME NWE, ALADIN MED and ALADIN EUR. The observational dataset COMEPHORE shows a higher amplitude in northeastern and central Corsica along the mountain range. Both AROME ALP and NWE simulations show a good agreement with the observations, but with a higher amplitude for high elevations (especially found in the AROME ALP simulation), while both ALADIN simulations are unable to capture the observed amplitude.

Given the limitations of the radar coverage over Corsica due to the masking effect of the mountains, the amplitude of the diurnal cycle in COMEPHORE is probably underestimated. Despite this, high amplitude values are found over the mountain ranges, better captured by AROME simulations (especially for AROME NWE, MSSS = 0.43). Thus, AROME simulations are probably closer to reality than what it seems from the comparison with COMEPHORE in most locations, especially on the west side of the island where there was no radar until recently.

Another important feature of the diurnal cycle is the time of maximum precipitation shown in Fig. 8. This feature is partially captured by the model simulations and is generally well simulated over the inland Corsica (in blueish) with a maximum in the early afternoon ($\sim$ 1400 UTC). However, it widely varies along the coasts from north to south and from east to west with different peak times, especially for the ALADIN simulations that cannot capture the timing near the coasts. Again here, the AROME simulations produce a time of maximum of the diurnal cycle that is in better agreement with the observation (COMEPHORE) than those of ALADIN, especially near the coasts.
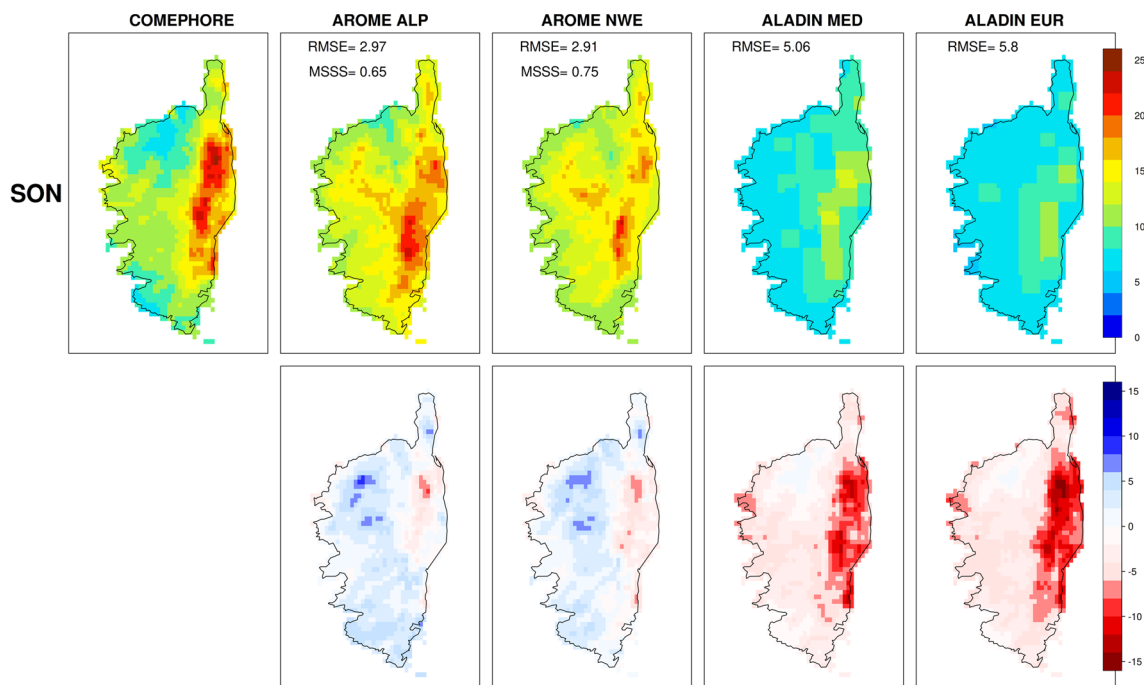
4.4 Hourly precipitation extremes

Located in a region of high cyclone track density, Corsica is often affected by Mediterranean HPEs from September to December. The 99.9th percentile of hourly precipitation is commonly used to identify significant accumulations of precipitation for sub-daily duration over localised areas.

Figure 9 shows the spatial distribution of hourly precipitation extremes in autumn. The observed hourly precipitation extremes in COMEPHORE (first column) are situated along the east coast of Corsica, exceeding locally 20 mm/h. When compared to the observations, the AROME simulations show a very good representation of the hourly extremes in autumn (MSSS > 0.65), while the ALADIN simulations are not able to reproduce them.

The absolute biases are indicated to quantify differences between model simulations and COMEPHORE data (second row of Fig. 9). Negative biases (in red), indicating an underestimation, are found for the ALADIN simulations (RMSE > 5 compared to the RMSE below 3 for AROME), especially in eastern Corsica. In addition, the statistical significance at the 90% confidence level of these biases was calculated using a bootstrapping method of 100 samplings and results confirm that the largest biases are statistically significant (see Fig. SM 1). These also confirm an added value of AROME compared to ALADIN for the simulation of hourly precipitation extremes, especially during the wettest season.

4.5 Probability density function of hourly precipitation

To gain further insight into the ability of these models to simulate the whole distribution of hourly precipitation during the wettest months (i.e. SON), the probability density function (PDF) is used. The PDF of hourly precipitation

Fig. 9 Spatial distribution of the 99.9th percentile of hourly precipitation (mm/h) in autumn for COMEPHORE, AROME ALP, AROME NWE, ALADIN MED and ALADIN EUR, with the corresponding RMSE and MSSS values (first row). The absolute differences between the model simulations and the observational dataset COMEPHORE (mm/h) with positive biases in blue and negative biases in red (second row)

(pr > 0.2 mm/h) for the observations and the model simulations in autumn and computed for eight locations in Corsica are shown in Fig. 10. Observed PDFs present higher intensities on the eastern coast, in particular for Solenzara and Bastia, as already seen in Sect. 4.4. The PDFs are overall better reproduced by AROME ALP (red line) and AROME NWE (red dotted line) simulations. This is particularly clear for the tail of the distributions (i.e. higher precipitation intensity). Meanwhile, ALADIN MED (blue line) and ALADIN EUR (blue dotted line) fail to capture the rare and most intense precipitation. For example, ALADIN simulates an hourly precipitation maximum of around 20 mm/h for Cap Corse, Figari and Solenzara while AROME simulates a maximum of around 70 mm/h for Solenzara.

4.6 Characterization of precipitation events

Commonly used in hydrology, the Intensity-Duration-Frequency (IDF) plot represents the relationship between the intensity, duration, and frequency (return period) of rainfall. An adaptation of this relationship is used here to test the models' ability to reproduce the intensity of precipitation events for different durations. Here, a precipitation event is defined as the accumulation of precipitation equal to or higher than 0.2 mm in at least one hour (i.e.

pr ≥ 0.2 mm/h). In addition, the frequency for each duration and intensity interval is computed in percentage.

Figure 11 shows the IDF plots for autumn and for three locations: Ajaccio, Sampolo and Solenzara, using weather station data, COMEPHORE data, AROME ALP, AROME NWE, ALADIN MED and ALADIN MED simulations. IDF plots from the observations (weather station and COMEPHORE) show that the most frequent events are associated with the shortest duration and the lowest intensities. While more intense events are much less frequent, lasting between 9 to 48 h. Again here, some differences can be seen between the eastern and western parts of Corsica, with more intense events (with longer lifetimes and higher cumulative precipitation totals) at the Solenzara station on the east coast. The IDF plots are better reproduced by the AROME ALP (third row) and AROME NW (fourth row) simulations while both ALADIN simulations tend to underestimate the intensity and overestimate the duration (i.e. precipitation events lasting up to 96 h).

No significant differences between the results of AROME ALP and AROME NWE can be seen so far, as both AROME simulations show similar conclusions with slight differences. In some cases, AROME ALP seems a little better than AROME NWE when compared with the observations. This could be potentially explained by the fact that spectral
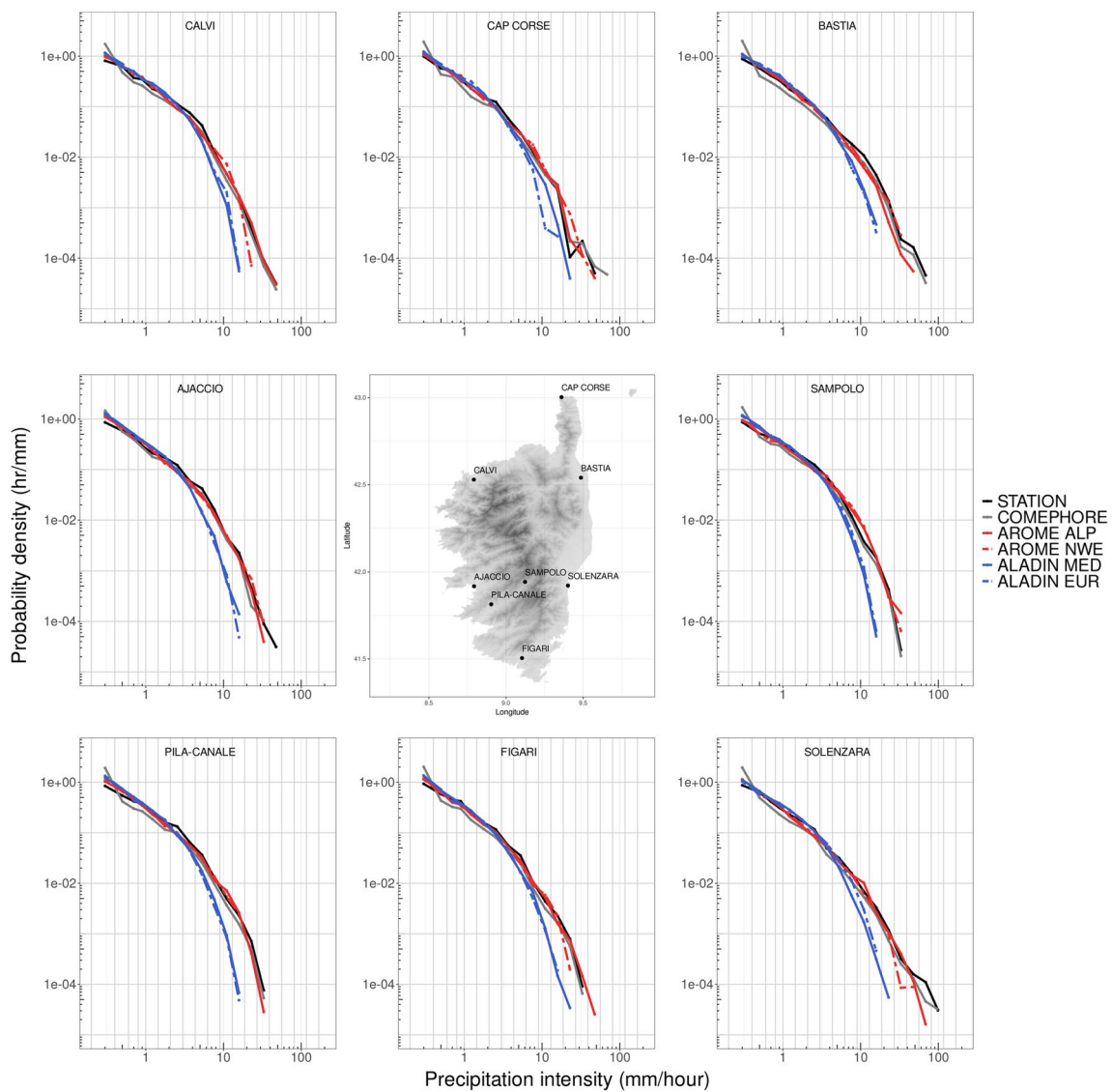
Fig. 10 Probability Density Function (PDF) of hourly precipitation for eight locations: Calvi, Ajaccio, Pila-Canale and Figari (western Corsica), Cap Corse, Bastia and Solenzara (eastern Corsica) and Sampolo (central and mountainous Corsica) for the STATION (black line), COMEPHORE (grey line), AROME ALP (red line), AROME NWE (red dotted line), ALADIN MED (blue) and ALADIN EUR (blue dotted line)

nudging is used in ALADIN MED, the driving field of AROME ALP, and also that Corsica is close to the lateral boundaries of the AROME NWE domain. The same conclusion can be drawn from the comparison between ALADIN MED and ALADIN EUR. For the sake of simplicity, the following analysis will consider only the results of the AROME ALP and ALADIN MED simulations, since these models have shown better consistencies with observations. This improvement is probably related to the spectral nudging technique used in ALADIN MED forcing AROME ALP and a better location of Corsica in the centre of the domain.

4.7 Local winds: sea–land and valley–mountain breezes

The largest land–sea temperature contrasts in Corsica occur during the summer season caused by daytime heating and nighttime cooling. The land warms and cools faster than the ocean due to the lower heat capacity of the continental surface compared to water. In the afternoon and evening, when the land is warmer than the sea, a sea breeze (from the sea toward the land) takes place. On the opposite, during the night and in the morning, when the land is colder than

Fig. 11 Intensity-Duration-Frequency diagrams for precipitation events in autumn for three locations: Ajaccio, Sampolo and Solenzara and for the corresponding weather station, COMEPHORE, AROME ALP, AROME NWE, ALADIN MED and ALADIN EUR. The number of precipitation events (pr ≥ 0.2 mm/h) is indicated at the top of each figure
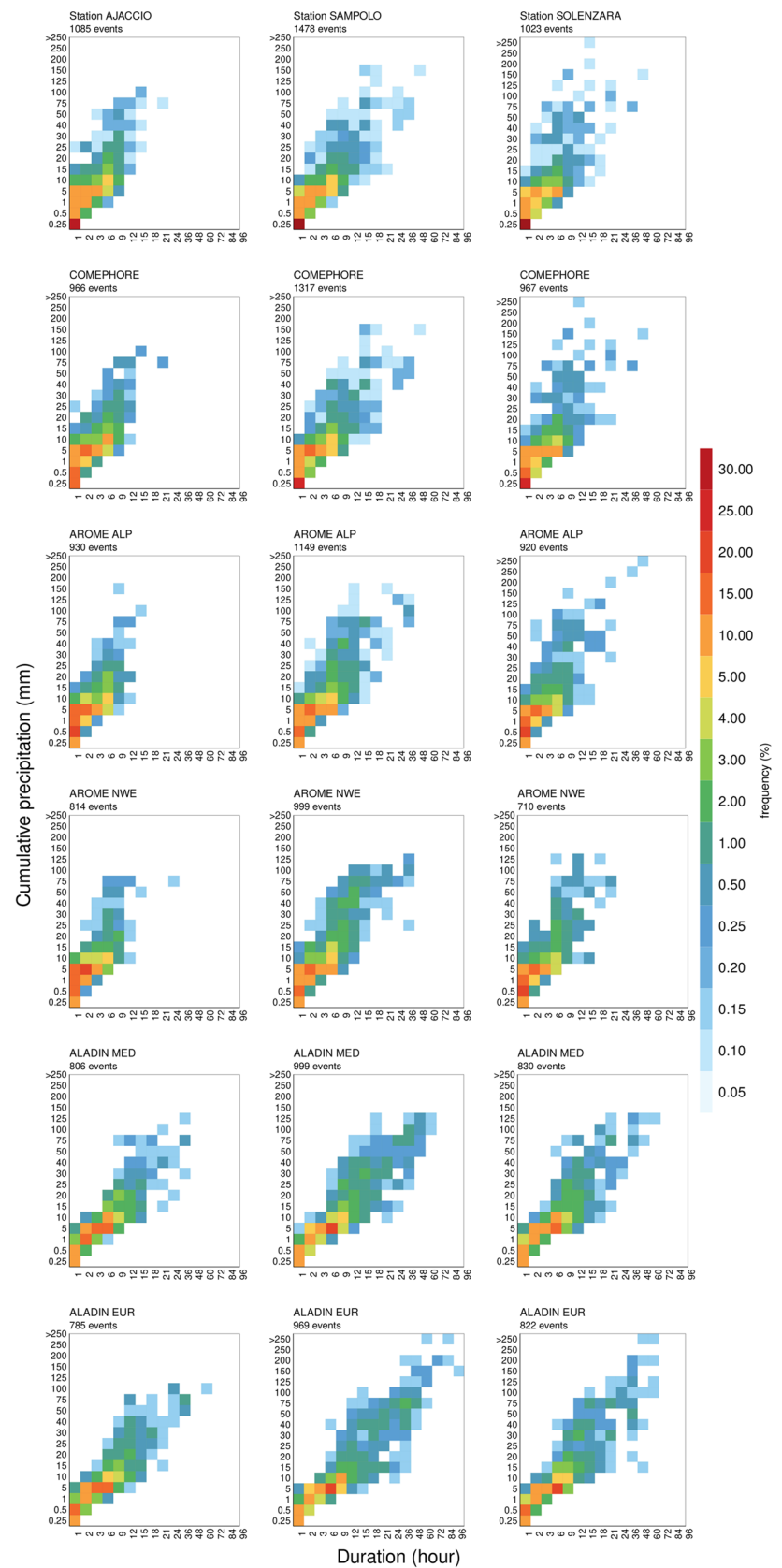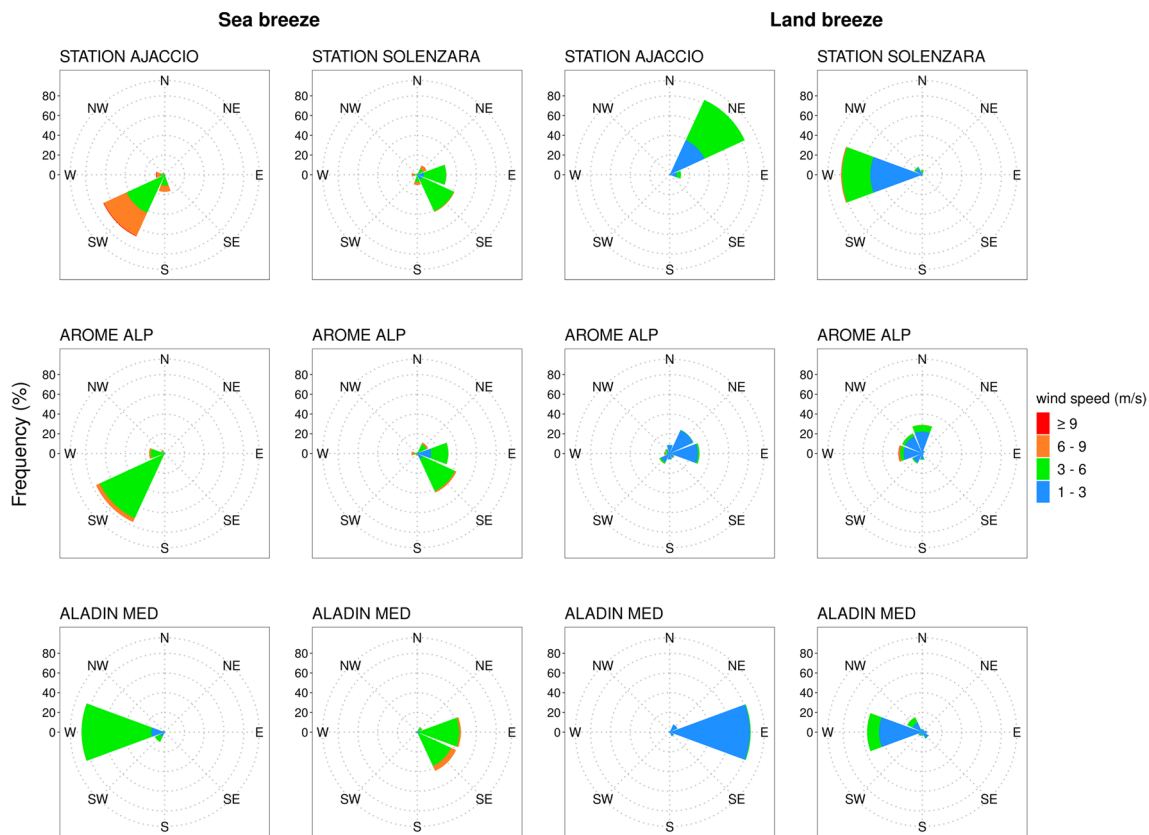
Fig. 12 Wind roses of the summer daytime sea breeze (1100 to 1400 UTC) and the nighttime land breeze (2300 to 0200 UTC) for the Ajaccio and Solenzara weather stations (top row), AROME ALP (middle row) and ALADIN MED (bottom row) simulations

the sea, a land breeze from the land toward the sea unfolds. Wind roses are commonly used to display wind breeze characteristics in terms of the predominant direction, wind speed, and associated frequency.

Figure 12 illustrates summer wind breezes for two coastal locations in Corsica: Ajaccio (middle of the west coast) and Solenzara (middle of the east coast). Mean wind fields of instantaneous wind speeds are computed from a 4-h interval in which the observed sea (from 1100 to 1400 UTC) and land (from 2300 to 0200 UTC) breezes are well established. Observed daytime sea breeze (columns on the left) and the nighttime land breeze (columns on the right) are compared with simulations in AROME ALP (second row), and ALA-DIN MED (third row).

For the west coast (in Ajaccio), a daytime sea breeze is observed with a predominant SW wind direction with a wind speed of up to 9 m/s. Then during the night, this circulation is reversed with a prevailing NE wind direction, but with a weaker wind speed intensity (up to 6 m/s). AROME ALP is able to well reproduce the daytime sea breeze despite an underestimation of the intensity. However, for the nighttime land breeze, the performance of AROME ALP is limited and it tends to underestimate both the intensity of predominant

winds and to simulate a wider range of directions, with predominant E and NE directions. On the other hand, ALADIN MED simulation shows an overall underestimation of wind intensity and a systematic shift in direction with dominant W (for sea breeze) and E (for land breeze) directions that are not in agreement with those observed. The difference between AROME and ALADIN wind breeze orientation is probably related to the topography which is better represented by AROME at 2.5 km able to reproduce the complex coastline effect and the Gulf of Ajaccio, whereas ALADIN at 12.5 km has a straight north–south coast (see Fig. 1c).

On the east coast (i.e. Solenzara), the observed sea breeze shows a SE direction that is slightly weaker compared to Ajaccio. Then, at nighttime, the main wind direction changes to the W direction. The daytime sea breeze is well reproduced by both AROME ALP and ALADIN MED. However, the land breeze is better reproduced by ALADIN MED showing a predominant W wind direction as observed while AROME ALP shows wind directions that are more spread from N, NW and W.

The local configuration of sea and land breezes was also investigated over central Corsica comparing AROME ALP and ALADIN MED simulations to observations from five

Fig. 13 Wind speed and direction during the summer daytime (from 1100 to 1400 UTC, on the left) sea breeze and nighttime (from 2300 to 0200 UTC, on the right) land breeze after subtracting the synoptic wind over central Corsica for **a** five weather stations (top row), **b** AROME ALP (middle row) and **c** ALADIN MED (bottom row). The weather stations are indicated with white dots in the AROME and ALADIN plots. The relief in Corsica is indicated by grey isolines every 500 m
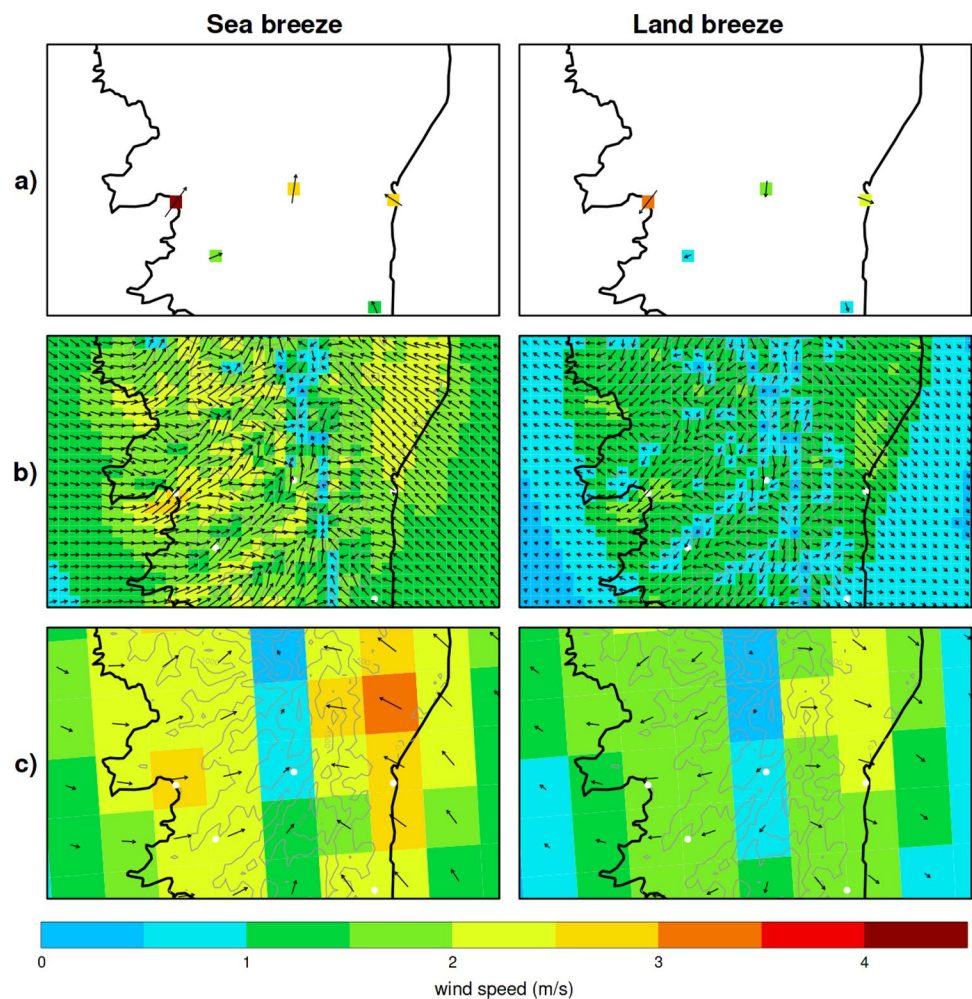
weather stations. The daily mean wind speed and direction (i.e. the synoptic component) is subtracted from a 4-h mean wind speed and direction to indicate wind anomalies as breezes. This 4-h interval corresponds to the occurrence of well-established daytime sea breezes (1100 to 1400 UTC) and nighttime land breezes (2300 to 0200 UTC). Figure 13 shows composites of the mean wind speed and direction after subtracting the synoptic component. While available weather stations provide a limited spatial representation of daytime sea breezes with strong intensities on the western coast and nighttime land breezes with weaker intensities, ALADIN MED simulations show a good but less detailed configuration of the breezes and AROME ALP simulations generate a continuous spatial representation of wind fields that is probably more realistic. Both wind direction and intensity are better reproduced by AROME ALP. Taking advantage of the high resolution of AROME ALP, it is also possible to identify the extension of the sea breeze on the western coast. Figure 13b illustrates how the sea breeze from the western coast penetrates inland Corsica interacting with

valley winds blowing in the same direction to then converge on the mountain range top. During summer, the extended sea breeze seems to be mainly responsible for triggering moist convection at the top of the mountain range. Further analysis and results on wind circulations, precipitation and humidity can be found in Supplementary Material Section 1.3.

5 Discussion and conclusions

This paper presents the evaluation of two 19-year hindcast simulations of the 2.5-km horizontal resolution CP-RCM AROME over the mountainous island of Corsica, which constitutes an ideal testbed for medium-sized Mediterranean islands. In this evaluation, the CP-RCM AROME is compared to high-resolution observational datasets (e.g. COMEPHORE, PRESCILIA and weather stations) and to the two driving RCM ALADIN simulations with a 12.5-km grid resolution.

The main objectives of this study included:

- to identify the added value of the CP-RCM AROME in the representation of key features of precipitation,
- to investigate the representation of local winds, their interaction with the local relief and their influence on the formation of summer orographic precipitation.

The first part of this work found that observed precipitation features of daily precipitation (i.e. the annual and seasonal mean, extremes, and their spatial distribution) are overall well reproduced by both CP-RCMs and RCMs. The CP-RCM AROME shows an improved representation of the annual cycle compared to RCM ALADIN simulations. Nonetheless, the spatial distribution of daily precipitation extremes shows higher precipitation intensities over localised areas at high elevations (along the mountain ranges). Such localised differences found in the CP-RCM have motivated our interest in the study of local-scale processes at sub-daily time scales.

The second part has focused on the representation of key features of local precipitation, which is much better simulated by the CP-RCM AROME. The summer diurnal cycle of precipitation i.e. the amplitude and time of maximum precipitation, mainly found in central Corsica are well reproduced. Despite a 1–2 h early peak of maximum precipitation, the afternoon peak only found at high elevations is better reproduced by the CP-RCM AROME simulations compared to ALADIN simulations which show a less intense and more even-distributed peak of precipitation. This improvement in AROME is probably related to the higher resolution in the model and its capacity to better resolve localised convection at high altitudes. The spatial distribution of hourly precipitation extremes (mainly found along the east coast of Corsica, where COMEPHORE is more reliable at lower altitudes and due to the presence of a weather radar since 2003) is well captured by the CP-RCM AROME, but not reproduced by the RCM ALADIN. In addition, due to their distinct nature, the observed spatial distribution of hourly precipitation extremes (i.e. on the east coast) is different to the one of daily mean precipitation (i.e. along the mountain ranges, where COMEPHORE is known to be less reliable). The CP-RCM AROME is skilful in differentiating such spatial characteristics, increasing confidence that the model shows a good performance.

The analysis of the PDF of hourly precipitation in autumn shows that AROME simulations present a good agreement, especially for the less frequent and more intense precipitation whereas the ALADIN simulations are not able to reproduce. The IDF of precipitation events is better represented by the CP-RCM AROME, particularly at three locations: Ajaccio (west coast), Sampolo (centre) and Solenzara (east coast). Although AROME and ALADIN simulations are able to reproduce events with high

amounts of precipitation, ALADIN tends to overestimate its duration having as a result longer and unrealistic precipitation events.

In the last part, the representation of local wind circulation and its further implication in the summer diurnal cycle of precipitation was investigated. Sea breeze circulations occur just after noon mainly during summer along the western and eastern coasts of Corsica. A stronger sea breeze is mostly observed over the western coast of Corsica, compared to a slightly weaker land breeze found after midnight. These general features of breeze circulations are better captured by the CP-RCM AROME.

Although both AROME simulations show a better performance than those of ALADIN, AROME ALP has a slightly better performance. The most important difference between the two CP-RCM AROME simulations comes from the spectral nudging that is relaxing the large scales of the atmosphere towards that of the driving ERA-Interim for the RCM ALADIN simulation performed over the MED-CORDEX domain that is forcing the AROME ALP domain. That additional large-scale forcing might reduce the biases of the RCM ALADIN simulation and also those of the AROME ALP simulation. The proximity of CORSICA to the lateral boundaries of the AROME NWE domain can also explain some underestimations of precipitation due to a too-short spatial spin-up. However, further analysis would be needed to fairly compare the two simulations which is out of the scope of this study.

The added value of the CP-RCM AROME compared to the RCM ALADIN was mainly found for the representation of:

- The annual cycle of precipitation with AROME ALP and AROME NWE values closer to the observations, although some overestimation.
- The summer diurnal cycle of precipitation which was only found at high elevations.
- The location and intensity of hourly precipitation extremes (99.9th percentile) on the eastern coast of Corsica during the wettest season (i.e. autumn).
- The tail of the probability density functions (i.e. the less frequent, but more intense precipitation) showing that the most intense hourly precipitation extremes are well reproduced.
- The IDF of autumn precipitation events is better represented by the CP-RCM with shorter and more intense events that match those observed.
- The daytime sea breeze is better represented in terms of the predominant wind direction and wind intensity.

This study faces some limitations impacting the interpretation of our analysis:

– The evaluation of climate models, in particular, at the kilometre resolution, relies on high-resolution and high-quality observations. However, as for many mountainous regions, hourly data from weather stations at higher altitudes in Corsica are scarce and discontinuous and radar data quality is also affected by masking effect from mountains. These limitations do not allow us to draw any definitive conclusion about the wet precipitation bias, mainly for monthly and annual accumulations, found in AROME over mountain ranges in Corsica, which could be linked to an underestimation of precipitation in the gridded precipitation datasets.

– For narrow coastal areas such as Cap Corse (north of Corsica), the selection of the neighbouring grid cell can be challenging as the performance of the model is sensitive to the grid cell location, land-surface fraction and altitude. This could affect in particular results from ALADIN due to its coarse resolution.

– In this study, monthly SSTs were used from interpolated ERA-Interim SSTs (around 80 km). This could explain some biases found in the representation of intense precipitation and breeze circulations, as fine-scale interactions between the ocean and atmosphere, especially near the Corsica coasts, could be misrepresented.

– Despite the 2.5 km horizontal resolution of the CP-RCM AROME, sub-grid phenomena (e.g. shallow convection) are still parameterised, affecting the representation of some local-scale atmospheric processes over the island. This representation could be further improved by higher-resolution models but this remains to be determined.

Some future recommendations include:

– Long records of high-quality and high-resolution observations as promoted by the TEAMx programme (http://www.teamx-programme.org/) over the Alps could help to evaluate high-resolution climate simulation and understand better local scale atmospheric dynamics.

– For the study of the processes involved in Mediterranean HPEs, hourly observations of precipitable water, wind, temperature and humidity in the lower layers are required.

– Increasing the spatial and temporal resolution of sea surface conditions forcing the CP-RCM AROME could improve the representation of ocean and atmosphere exchanges near coastal areas. Sensitivity studies could bring insight into the benefits of increasing SST resolution.

Further research is still needed to improve our understanding of other extreme phenomena affecting Corsica, such as heatwaves and strong winds, and how these are represented in high-resolution climate models. For example,

the new climate simulations using AROME will include lightning diagnosis that would be compared with the electrical activity measured during the EXAEDRE campaign.

Our main findings show that high-resolution climate modelling is required to realistically reproduce key meteorological phenomena over islands with complex orography and land–sea contrasts. These increase our confidence in CP-RCMs to investigate future climate projections for Corsica and islands with complex terrain. As future projections in precipitation have shown an opposite signal of change over high altitudes between RCMs and GCMs (Giorgi et al. 2016), the use of CP-RCM can provide a new insight.

Declarations

References

Abbs DJ, Physick WL (1992) Sea-breeze observations and modelling: a review. Aust Meteorol Mag 41:7

Adinolfi M, Raffa M, Reder A, Mercogliano P (2021) Evaluation and expected changes of summer precipitation at convection permitting scale with COSMO-CLM over alpine space. Atmosphere. https://doi.org/10.3390/atmos12010054

Argüeso D, Di Luca A, Evans JP (2016) Precipitation over urban areas in the western Maritime Continent using a convection-permitting model. Clim Dyn 47(3–4):1143–1159. https://doi.org/10.1007/s00382-015-2893-6

Argüeso D, Romero R, Homar V (2020) Precipitation features of the Maritime Continent in parameterized and explicit convection models. J Clim 33(6):2449–2466. https://doi.org/10.1175/JCLI-D-19-0416.1

Armon M, Marra F, Enzel Y, Rostkier-Edelstein D, Morin E (2020) Radar-based characterisation of heavy precipitation in the eastern Mediterranean and its representation in a convection-permitting model. Hydrol Earth Syst Sci 24(3):1227–1249. https://doi.org/10.5194/hess-24-1227-2020

Azorin-Molina C, Chen D, Tijm S, Baldi M (2011) A multi-year study of sea breezes in a Mediterranean coastal site: Alicante (Spain). Int J Climatol 31(3):468–486. https://doi.org/10.1002/joc.2064

Ban N, Schmidli J, Schär C (2014) Evaluation of the convection-resolving regional climate modeling approach in decade-long simulations. J Geophys Res: Atmos 119(13):7889–7907. https://doi.org/10.1002/2014JD021478

Ban N, Schmidli J, Schär C (2015) Heavy precipitation in a changing climate: does short-term summer precipitation increase faster? Geophys Res Lett 42(4):1165–1172. https://doi.org/10.1002/2014GL062588

Ban N, Caillaud C, Coppola E, Pichelli E, Sobolowski S, Adinolfi M, Ahrens B, Alias A, Anders I, Bastin S, Belušić D, Berthou S, Brisson E, Cardoso RM, Chan SC, Christensen OB, Fernández J, Fita L, Frisius T, Gašparac G, Giorgi F, Goergen K, Haugen JE, Hodnebrog Kartsios S, Katragkou E, Kendon EJ, Keuler K, Lavin-Gullon A, Lenderink G, Leutwyler D, Lorenz T, Maraun D, Mercogliano P, Milovac J, Panitz HJ, Raffa M, Remedio AR, Schär C, Soares PM, Srnec L, Steensen BM, Stocchi P, Tölle MH, Truhetz H, Vergara-Temprado J, de Vries H, Warrach-Sagi K, Wulfmeyer V, Zander MJ (2021) The first multi-model ensemble of regional climate simulations at kilometer-scale resolution, part I: evaluation of precipitation. Clim Dyn 57(1–2):275–302. https://doi.org/10.1007/s00382-021-05708-w

Barthlott C, Kirshbaum DJ (2013) Sensitivity of deep convection to terrain forcing over Mediterranean islands. Q J R Meteorol Soc 139(676):1762–1779. https://doi.org/10.1002/qj.2089

Barthlott C, Adler B, Kalthoff N, Handwerker J, Kohler M, Wieser A (2014) The role of Corsica in initiating nocturnal offshore convection. Q J R Meteorol Soc. https://doi.org/10.1002/qj.2415

Berthou S, Kendon EJ, Chan SC, Ban N, Leutwyler D, Schär C, Fosser G (2020) Pan-European climate at convection-permitting scale: a model intercomparison study. Clim Dyn 55(1–2):35–59. https://doi.org/10.1007/s00382-018-4114-6

Birch CE, Marsham JH, Parker DJ, Taylor CM (2014) The scale dependence and structure of convergence fields preceding the initiation of deep convection. Geophys Res Lett 41(13):4769–4776. https://doi.org/10.1002/2014GL060493

Bouin MN, Lebeaupin Brossier C (2020) Surface processes in the 7 November 2014 medicane from air–sea coupled high-resolution numerical modelling. Atmos Chem Phys 20(11):6861–6881. https://doi.org/10.5194/acp-20-6861-2020

Brockhaus P, Lüthi D, Schär C (2008) Aspects of the diurnal cycle in a regional climate model. Meteorologische Zeitschrift 17(4):433–443. https://doi.org/10.1127/0941-2948/2008/0316

Caillaud C, Somot S, Alias A, Bernard-Bouissières I, Fumière Q, Laurantin O, Seity Y, Ducrocq V (2021) Modelling Mediterranean heavy precipitation events at climate scale: an object-oriented evaluation of the CNRM-AROME convection-permitting regional climate model. Clim Dyn 56(5–6):1717–1752. https://doi.org/10.1007/s00382-020-05558-y

Chan SC, Kendon EJ, Fowler HJ, Blenkinsop S, Ferro CAT, Stephenson DB (2013) Does increasing the spatial resolution of a regional climate model improve the simulated daily precipitation? Clim Dyn 41(5–6):1475–1495. https://doi.org/10.1007/s00382-012-1568-9

Coppin D, Bellon G (2019a) Physical mechanisms controlling the offshore propagation of convection in the tropics: 1. Flat island. J Adv Model Earth Syst 11(9):3042–3056. https://doi.org/10.1029/2019MS001793

Coppin D, Bellon G (2019b) Physical mechanisms controlling the offshore propagation of convection in the tropics: 2. Influence of topography. J Adv Model Earth Syst 11(10):3251–3264. https://doi.org/10.1029/2019MS001794

Coppola E, Sobolowski S, Pichelli E, Raffaele F, Ahrens B, Anders I, Ban N, Bastin S, Belda M, Belusic D, Caldas-Alvarez A, Cardoso RM, Davolio S, Dobler A, Fernandez J, Fita L, Fumiere Q, Giorgi F, Goergen K, Güttler I, Halenka T, Heinzeller D, Hodnebrog Jacob D, Kartsios S, Katragkou E, Kendon E, Khodayar S, Kunstmann H, Knist S, Lavín-Gullón A, Lind P, Lorenz T, Maraun D, Marelle L, van Meijgaard E, Milovac J, Myhre G, Panitz HJ, Piazza M, Raffa M, Raub T, Rockel B, Schär C, Sieck K, Soares PMM, Somot S, Srnec L, Stocchi P, Tölle MH, Truhetz H, Vautard R, de Vries H, Warrach-Sagi K (2020) A first-of-its-kind multi-model convection permitting ensemble for investigating convective phenomena over Europe and the Mediterranean. Clim Dyn 55(1–2):3–34. https://doi.org/10.1007/s00382-018-4521-8

Cronin TW, Emanuel KA, Molnar P (2015) Island precipitation enhancement and the diurnal cycle in radiative-convective equilibrium. Q J R Meteorol Soc 141(689):1017–1034. https://doi.org/10.1002/qj.2443

Drobinski P, Ducrocq V, Alpert P, Anagnostou E, Béranger K, Borga M, Braud I, Chanzy A, Davolio S, Delrieu G, Estournel C, Boubrahmi NF, Font J, Grubišić V, Gualdi S, Homar V, Ivančan-Picek B, Kottmeier C, Kotroni V, Lagouvardos K, Lionello P, Llasat MC, Ludwig W, Lutoff C, Mariotti A, Richard E, Romero R, Rotunno R, Roussot O, Ruin I, Somot S, Taupier-Letage I, Tintore J, Uijlenhoet R, Wernli H (2014) HyMeX: A 10-year multidisciplinary program on the mediterranean water cycle. Bullet Amer Meteorol Soc 95(7):1063–1082. https://doi.org/10.1175/BAMS-D-12-00242.1

Ducrocq V, Nuissier O, Ricard D, Lebeaupin C, Thouvenin T (2008) A numerical study of three catastrophic precipitating events over southern France. II: mesoscale triggering and stationarity factors. Q J R Meteorol Soc 134(630):131–145. https://doi.org/10.1002/qj.199

Ducrocq V, Braud I, Davolio S, Ferretti R, Flamant C, Jansa A, Kalthoff N, Richard E, Taupier-Letage I, Ayral PA, Belamari S, Berne A, Borga M, Boudevillain B, Bock O, Boichard JL, Bouin MN, Bousquet O, Bouvier C, Chiggiato J, Cimini D, Corsmeier U, Coppola L, Cocquerez P, Defer E, Delanoë J, Di Girolamo P, Doerenbecher A, Drobinski P, Dufournet Y, Fourrié N, Gourley JJ, Labatut L, Lambert D, Le Coz J, Marzano FS, Molinié G, Montani A, Nord G, Nuret M, Ramage K, Rison W, Roussot O, Said F, Schwarzenboeck A, Testor P, Van Baelen J, Vincendon B, Aran M, Tamayo J (2014) HyMeX-SOP1: the field campaign dedicated to heavy precipitation and flash flooding in the northwestern Mediterranean. Bull Am Meteorol Soc 95(7):1083–1100. https://doi.org/10.1175/BAMS-D-12-00244.1

Dutheil C, Menkes C, Lengaigne M, Vialard J, Peltier A, Bador M, Petit X (2021) Fine-scale rainfall over New Caledonia under climate change. Clim Dyn 56(1–2):87–108. https://doi.org/10.1007/s00382-020-05467-0

Erdmann F, Defer E, Caumont O, Blakeslee RJ, Pédeboy S, Coquillat S (2020) Concurrent satellite and ground-based lightning observations from the Optical Lightning Imaging Sensor (ISS-LIS), the low-frequency network Meteorage and the SAETTA Lightning Mapping Array (LMA) in the northwestern Mediterranean region. Atmos Meas Techn 13(2):853–875. https://doi.org/10.5194/amt-13-853-2020

Expósito FJ, González A, Pérez JC, Díaz JP, Taima D (2015) High-resolution future projections of temperature and precipitation in the Canary Islands. J Clim 28(19):7846–7856. https://doi.org/10.1175/JCLI-D-15-0030.1

Fery L, Faranda, D (2024) Analysing 23 years of warm-season derechos in France: a climatology and investigation of synoptic and environmental changes. Weather Clim Dynam 5:439–461. https://doi.org/10.5194/wcd-5-439-2024

Flaounas E, Aragão L, Bernini L, Dafis S, Doiteau B, Flocas H, Gray SL, Karwat A, Kouroutzoglou J, Lionello P, Miglietta MM, Pantillon F, Pasquero C, Patlakas P, Picornell M, Porcù F, Priestley MD, Reale M, Roberts MJ, Saaroni H, Sandler D, Scoccimarro E, Sprenger M, Ziv B (2023) A composite approach to produce reference datasets for extratropical cyclone tracks: application to Mediterranean cyclones. Weather Clim Dyn 4(3):639–661. https://doi.org/10.5194/WCD-4-639-2023

Fosser G, Khodayar S, Berg P (2015) Benefit of convection permitting climate model simulations in the representation of convective precipitation. Clim Dyn 44(1–2):45–60. https://doi.org/10.1007/s00382-014-2242-1

Fumière Q, Déqué M, Nuissier O, Somot S, Alias A, Caillaud C, Laurantin O, Seity Y (2020) Extreme rainfall in Mediterranean France during the fall: added value of the CNRM-AROME Convection-Permitting Regional Climate Model. Clim Dyn 55(1–2):77–91. https://doi.org/10.1007/s00382-019-04898-8

Furberg M, Steyn DG, Baldi M (2002) The climatology of sea breezes on Sardinia. Int J Climatol 22(8):917–932. https://doi.org/10.1002/joc.780

Giorgi F (2006) Climate change hot-spots. Geophys Res Lett. https://doi.org/10.1029/2006GL025734

Giorgi F (2019) Thirty years of regional climate modeling: where are we and where are we going next? J Geophys Res: Atmos 124(11):5696–5723. https://doi.org/10.1029/2018JD030094

Giorgi F, Torma C, Coppola E, Ban N, Schär C, Somot S (2016) Enhanced summer convective rainfall at Alpine high elevations in response to climate warming. Nat Geosci 9(8):584–589. https://doi.org/10.1038/ngeo2761

González-Alemán JJ, Insua-Costa D, Bazile E, González-Herrero S, Miglietta MM, Groenemeijer P, Donat MG (2023) Anthropogenic warming had a crucial role in triggering the historic and destructive Mediterranean derecho in summer 2022. Bull Am Meteorol Soc 104(8):E1526–E1532. https://doi.org/10.1175/BAMS-D-23-0119.1

Guérémy JF (2011) A continuous buoyancy based convection scheme: one- and three-dimensional validation. Tellus A: Dyn Meteorol Oceanogr 63(4):687. https://doi.org/10.1111/j.1600-0870.2011.00521.x

Hassim ME, Lane TP, Grabowski WW (2016) The diurnal cycle of rainfall over New Guinea in convection-permitting WRF simulations. Atmos Chem Phys 16(1):161–175. https://doi.org/10.5194/acp-16-161-2016

Im ES, Eltahir EAB (2018) Simulation of the diurnal variation of rainfall over the western Maritime Continent using a regional climate model. Clim Dyn 51(1–2):73–88. https://doi.org/10.1007/s00382-017-3907-3

Kendon EJ, Roberts NM, Senior CA, Roberts MJ (2012) Realism of rainfall in a very high-resolution regional climate model. J Clim 25(17):5791–5806. https://doi.org/10.1175/JCLI-D-11-00562.1

Kendon EJ, Roberts NM, Fowler HJ, Roberts MJ, Chan SC, Senior CA (2014) Heavier summer downpours with climate change revealed by weather forecast resolution model. Nat Clim Change 4(7):570–576. https://doi.org/10.1038/nclimate2258

Kendon EJ, Ban N, Roberts NM, Fowler HJ, Roberts MJ, Chan SC, Evans JP, Fosser G, Wilkinson JM (2017) Do convection-permitting regional climate models improve projections of future precipitation change? Bull Am Meteorol Soc 98(1):79–93. https://doi.org/10.1175/BAMS-D-15-0004.1

Khodayar S, Davolio S, Di Girolamo P, Lebeaupin Brossier C, Flaounas E, Fourrie N, Lee KO, Ricard D, Vie B, Bouttier F, Caldas-Alvarez A, Ducrocq V (2021) Overview towards improved understanding of the mechanisms leading to heavy precipitation in the western Mediterranean: lessons learned from HyMeX. Atmos Chem Phys 21(22):17051–17078. https://doi.org/10.5194/acp-21-17051-2021

Knerr I, Trachte K, Garel E, Huneau F, Santoni S, Bendix J (2020) Partitioning of large-scale and local-scale precipitation events by means of spatio-temporal precipitation regimes on Corsica. Atmosphere 11(4):417. https://doi.org/10.3390/atmos11040417

Kondo H (1990) A numerical experiment on the interaction between sea breeze and valley wind to generate the so-called "extended sea breeze". J Meteorol Soc Jpn 68(4):435–446. https://doi.org/10.2151/jmsj1965.68.4_435

Kottmeier C, Palacio-Sese P, Kalthoff N, Corsmeier U, Fiedler F (2000) Sea breezes and coastal jets in southeastern Spain. Int J Climatol 20(14):1791–1808. https://doi.org/10.1002/1097-0088(20001130)20:14<1791::AID-JOC574>3.0.CO;2-I

Lambert D, Mallet M, Ducrocq V, Dulac F, Gheusi F, Kalthoff N (2011) CORSiCA: a Mediterranean atmospheric and oceanographic observatory in Corsica within the framework of HyMeX and ChArMEx. Adv Geosci 26(1):125–131. https://doi.org/10.5194/adgeo-26-125-2011

Langhans W, Schmidli J, Fuhrer O, Bieri S, Schär C (2013) Long-term simulations of thermally driven flows and orographic convection at convection-parameterizing and cloud-resolving resolutions. J Appl Meteorol Climatol 52(6):1490–1510. https://doi.org/10.1175/JAMC-D-12-0167.1

Lebeaupin Brossier C, Ducrocq V, Giordani H (2008) Sensitivity of three Mediterranean heavy rain events to two different sea surface fluxes parameterizations in high-resolution numerical modeling. J Geophys Res 113(D21):D21109. https://doi.org/10.1029/2007JD009613

Leps N (2016) Influence of atmosphere–ocean interactions on deep convection over Corsica. PhD thesis

Lucas-Picher P, Argüeso D, Brisson E, Tramblay Y, Berg P, Lemonsu A, Kotlarski S, Caillaud C (2021) Convection-permitting modeling with regional climate models: latest developments and next steps. Wiley Interdiscip Rev: Clim Change. https://doi.org/10.1002/wcc.731

Lucas-Picher P, Brisson E, Caillaud C, Alias A, Nabat P, Lemonsu A, Poncet N, Cortés Hernandez VE, Michau Y, Doury A, Monteiro D, Somot S (2023) Evaluation of the convection-permitting regional climate model CNRM-AROME41t1 over Northwestern Europe. Clim Dyn. https://doi.org/10.1007/s00382-022-06637-y

Lundquist J, Hughes M, Gutmann E, Kapnick S (2019) Our skill in modeling mountain rain and snow is bypassing the skill of our observational networks. Bull Am Meteorol Soc 100(12):2473–2490. https://doi.org/10.1175/BAMS-D-19-0001.1

Luu LN, Vautard R, Yiou P, Soubeyroux JM (2022) Evaluation of convection-permitting extreme precipitation simulations for the south of France. Earth Syst Dyn 13(1):687–702. https://doi.org/10.5194/esd-13-687-2022

Mahrer Y, Pielke RA (1977) The effects of topography on sea and land breezes in a two-dimensional numerical model. Mon Weather Rev 105(9):1151–1162. https://doi.org/10.1175/1520-0493(1977)105

Meredith EP, Ulbrich U, Rust HW (2020) Subhourly rainfall in a convection-permitting model. Environ Res Lett 15(3):034031. https://doi.org/10.1088/1748-9326/ab6787

Michou M, Nabat P, Saint-Martin D, Bock J, Decharme B, Mallet M, Roehrig R, Séférian R, Sénési S, Voldoire A (2020) Present-day and historical aerosol and ozone characteristics in CNRM CMIP6 simulations. J Adv Model Earth Syst 12(1):e2019MS001816. https://doi.org/10.1029/2019MS001816

Monteiro D, Caillaud C, Samacoïts R, Lafaysse M, Morin S (2022) Potential and limitations of convection-permitting CNRM-AROME climate modelling in the French Alps. Int J Climatol. https://doi.org/10.1002/joc.7637

Morel B, Pohl B, Richard Y, Bois B, Bessafi M (2014) Regionalizing rainfall at very high resolution over La Réunion Island using a regional climate model. Mon Weather Rev 142(8):2665–2686. https://doi.org/10.1175/MWR-D-14-00009.1

Murata A, Sasaki H, Kawase H, Nosaka M (2017) Evaluation of precipitation over an oceanic region of Japan in convection-permitting regional climate model simulations. Clim Dyn 48(5–6):1779–1792. https://doi.org/10.1007/s00382-016-3172-x

Murphy AH (1988) Skill scores based on the mean square error and their relationships to the correlation coefficient. Mon Weather Rev 116(12):2417–2424. https://doi.org/10.1175/1520-0493(1988)116

Nabat P, Somot S, Mallet M, Chiapello I, Morcrette JJ, Solmon F, Szopa S, Dulac F, Collins W, Ghan S, Horowitz LW, Lamarque JF, Lee YH, Naik V, Nagashima T, Shindell D, Skeie R (2013) A 4-D climatology (1979–2009) of the monthly tropospheric aerosol optical depth distribution over the Mediterranean region from a comparative evaluation and blending of remote sensing and model products. Atmos Meas Tech 6(5):1287–1314. https://doi.org/10.5194/amt-6-1287-2013

Nabat P, Somot S, Cassou C, Mallet M, Michou M, Bouniol D, Decharme B, Drugé T, Roehrig R, Saint-Martin D (2020) Modulation of radiative aerosols effects by atmospheric circulation over the Euro-Mediterranean region. Atmos Chem Phys 20(14):8315–8349. https://doi.org/10.5194/acp-20-8315-2020

Nuissier O, Ducrocq V, Ricard D, Lebeaupin C, Anquetin S (2008) A numerical study of three catastrophic precipitating events over southern France. I: Numerical framework and synoptic ingredients. Q J R Meteorol Soc 134(630):111–130. https://doi.org/10.1002/qj.200

Nuissier O, Joly B, Joly A, Ducrocq V, Arbogast P (2011) A statistical downscaling to identify the large-scale circulation patterns associated with heavy precipitation events over southern France. Q J R Meteorol Soc 137(660):1812–1827. https://doi.org/10.1002/qj.866

Pichelli E, Coppola E, Sobolowski S, Ban N, Giorgi F, Stocchi P, Alias A, Belušić D, Berthou S, Caillaud C, Cardoso RM, Chan S, Christensen OB, Dobler A, de Vries H, Goergen K, Kendon EJ, Keuler K, Lenderink G, Lorenz T, Mishra AN, Panitz HJ, Schär C, Soares PM, Truhetz H, Vergara-Temprado J (2021) The first multi-model ensemble of regional climate simulations at kilometer-scale resolution part 2: historical and future simulations of precipitation. Clim Dyn 56(11–12):3581–3602. https://doi.org/10.1007/s00382-021-05657-4

Piriou JM, Redelsperger JL, Geleyn JF, Lafore JP, Guichard F (2007) An approach for convective parameterization with memory: separating microphysics and transport in grid-scale equations. J Atmos Sci 64(11):4127–4139. https://doi.org/10.1175/2007JAS2144.1

Prein AF, Langhans W, Fosser G, Ferrone A, Ban N, Goergen K, Keller M, Tölle M, Gutjahr O, Feser F, Brisson E, Kollet S, Schmidli J, Lipzig NPM, Leung R (2015) A review on regional convection-permitting climate modeling: demonstrations, prospects, and challenges. Rev Geophys 53(2):323–361. https://doi.org/10.1002/2014RG000475

Radu R, Déqué M, Somot S (2008) Spectral nudging in a spectral regional climate model. Tellus A: Dyn Meteorol Oceanogr 60(5):898. https://doi.org/10.1111/j.1600-0870.2008.00341.x

Rainaud R, Brossier CL, Ducrocq V, Giordani H (2017) High-resolution air–sea coupling impact on two heavy precipitation events in the Western Mediterranean. Q J R Meteorol Soc 143(707):2448–2462. https://doi.org/10.1002/qj.3098

Ricard D, Ducrocq V, Auger L (2012) A climatology of the mesoscale environment associated with heavily precipitating events over a northwestern Mediterranean area. J Appl Meteorol Climatol 51(3):468–488. https://doi.org/10.1175/JAMC-D-11-017.1

Rome S, Giorgetti JP (2006) Du climat de la montagne Corse et ses aleas. In: XIXème colloque de l'Association Internationale de Climatologie, Université Grenoble Alpes, p 6

Rome S, Giorgetti JP (2007) La montagne corse et ses caractéristiques climatiques. La Météorologie 8(59):39. https://doi.org/10.4267/2042/14846

Ruppert JH, Chen X (2020) Island rainfall enhancement in the Maritime Continent. Geophys Res Lett. https://doi.org/10.1029/2019GL086545

Ruppert JH, Zhang F (2019) Diurnal forcing and phase locking of gravity waves in the Maritime Continent. J Atmos Sci 76(9):2815–2835. https://doi.org/10.1175/JAS-D-19-0061.1

Ruti PM, Somot S, Giorgi F, Dubois C, Flaounas E, Obermann A, Dell'Aquila A, Pisacane G, Harzallah A, Lombardi E, Ahrens B, Akhtar N, Alias A, Arsouze T, Aznar R, Bastin S, Bartholy J, Béranger K, Beuvier J, Bouffies-Cloché S, Brauch J, Cabos W, Calmanti S, Calvet JC, Carillo A, Conte D, Coppola E, Djurdjevic V, Drobinski P, Elizalde-Arellano A, Gaertner M, Galàn P, Gallardo C, Gualdi S, Goncalves M, Jorba O, Jordà G, L'Heveder B, Lebeaupin-Brossier C, Li L, Liguori G, Lionello P, Maciàs D, Nabat P, Önol B, Raikovic B, Ramage K, Sevault F, Sannino G, Struglia MV, Sanna A, Torma C, Vervatis V (2016) Med-CORDEX initiative for Mediterranean climate studies. Bull Am Meteorol Soc 97(7):1187–1208. https://doi.org/10.1175/BAMS-D-14-00176.1

Scheffknecht P, Richard E, Lambert D (2016) A highly localized high-precipitation event over Corsica. Q J R Meteorol Soc 142(S1):206–221. https://doi.org/10.1002/qj.2795

Scheffknecht P, Richard E, Lambert D (2017) Climatology of heavy precipitation over Corsica in the period 1985–2015. Q J R Meteorol Soc 143(709):2987–2998. https://doi.org/10.1002/qj.3140

Seity Y, Malardel S, Hello G, Bénard P, Bouttier F, Lac C, Masson V (2011) The AROME-France convective-scale operational model. Mon Weather Rev 139(3):976–991. https://doi.org/10.1175/2010MWR3425.1

Seneviratne SI, Zhang X, Adnan M, Badi W, Dereczynski C, Di Luca A, Ghosh S, Iskandar I, Kossin J, Lewis S, Otto F, Pinto I, Satoh M, Vicente-Serrano SM, Wehner M, Zhou B (2021) Weather and climate extreme events in a changing climate. In: Masson-Delmotte V, Zhai P, Pirani A, Connors SL, Péan C, Berger S, Caud N, Chen Y, Goldfarb L, Gomis MI, Huang M, Leitzell K, Lonnoy E, Matthews JBR, Maycock TK, Waterfield T, Yelekçi O, Yu R, Zhou B (eds) Climate Change 2021: the physical science basis. Contribution of working group I to the sixth assessment report of the Intergovernmental Panel on Climate Change. Cambridge University Press, Cambridge and New York, pp 1513–1766. https://doi.org/10.1017/9781009157896.013

Soubeyroux JM, Lassègues P, Simon P, Canellas C (2019) La méthode Prescilia de spatialisation quotidienne des précipitations à partir de types de temps. In: XXXIIeme colloque annuel de l'Association Internationale de Climatologie, pp 517–522

Tabary P, Dupuy P, L'Henaff G, Gueguen C, Moulin L, Laurantin O, Merlier C, Soubeyroux JM (2011) A 10-year (1997–2006) reanalysis of Quantitative Precipitation Estimation over France: methodology and first results. In: International Association of Hydrological Sciences WUK (ed) Weather radar and hydrology. Exeter, pp 255–260

Trigo IF, Bigg GR, Davies TD (2002) Climatology of cyclogenesis mechanisms in the Mediterranean. Mon Weather Rev 130(3):549–569. https://doi.org/10.1175/1520-0493(2002)130<0549:COCMIT>2.0.CO;2

Vincent CL, Lane TP (2016) Evolution of the diurnal precipitation cycle with the passage of a Madden–Julian oscillation event through the Maritime Continent. Mon Weather Rev 144(5):1983–2005. https://doi.org/10.1175/MWR-D-15-0326.1

Wang Y, Geerts B, Liu C (2018) A 30-year convection-permitting regional climate simulation over the interior western United States. Part I: validation. Int J Climatol 38(9):3684–3704. https://doi.org/10.1002/joc.5527

Wei Y, Pu Z, Zhang C (2020) Diurnal cycle of precipitation over the Maritime Continent under modulation of MJO: perspectives from cloud-permitting scale simulations. J Geophys Res: Atmos. https://doi.org/10.1029/2020JD032529

Wu P, Yamanaka MD, Matsumoto J (2008) The formation of nocturnal rainfall offshore from convection over Western Kalimantan (Borneo) Island. J Meteorol Soc Jpn 86A:187–203. https://doi.org/10.2151/jmsj.86A.187

Zhang C, Wang Y, Hamilton K, Lauer A (2016) Dynamical downscaling of the climate for the Hawaiian Islands. Part II: projection for the late twenty-first century. J Clim 29(23):8333–8354. https://doi.org/10.1175/JCLI-D-16-0038.1

Zhu L, Meng Z, Zhang F, Markowski PM (2017) The influence of sea- and land-breeze circulations on the diurnal variability in precipitation over a tropical island. Atmos Chem Phys 17(21):13213–13232. https://doi.org/10.5194/acp-17-13213-2017

Zhu L, Bai L, Chen G, Sun YQ, Meng Z (2021) Convection initiation associated with ambient winds and local circulations over a tropical island in South China. Geophys Res Lett 48(16):e2021GL094382. https://doi.org/10.1029/2021GL094382